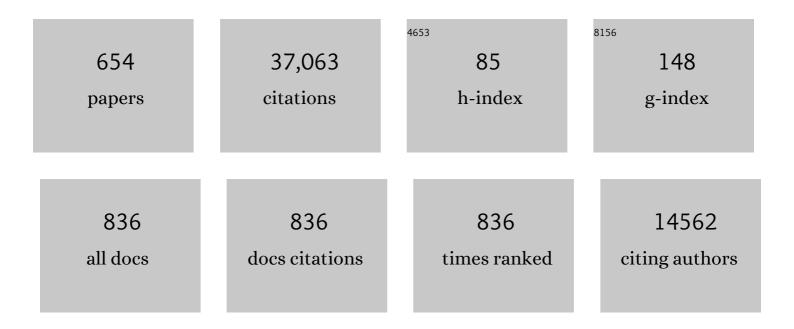
John P Burrows

List of Publications by Year in descending order

Source: https://exaly.com/author-pdf/5660461/publications.pdf Version: 2024-02-01



IOHN P RUDDOWS

#	Article	IF	CITATIONS
1	SCIAMACHY: Mission Objectives and Measurement Modes. Journals of the Atmospheric Sciences, 1999, 56, 127-150.	0.6	1,715
2	Increase in tropospheric nitrogen dioxide over China observed from space. Nature, 2005, 437, 129-132.	13.7	1,300
3	The Global Ozone Monitoring Experiment (GOME): Mission Concept and First Scientific Results. Journals of the Atmospheric Sciences, 1999, 56, 151-175.	0.6	1,105
4	The nitrate radical: Physics, chemistry, and the atmosphere. Atmospheric Environment Part A General Topics, 1991, 25, 1-203.	1.3	646
5	Measurements of molecular absorption spectra with the SCIAMACHY pre-flight model: instrument characterization and reference data for atmospheric remote-sensing in the 230–2380 nm region. Journal of Photochemistry and Photobiology A: Chemistry, 2003, 157, 167-184.	2.0	605
6	The Orbiting Carbon Observatory (OCO) mission. Advances in Space Research, 2004, 34, 700-709.	1.2	596
7	Halogens and their role in polar boundary-layer ozone depletion. Atmospheric Chemistry and Physics, 2007, 7, 4375-4418.	1.9	593
8	Global budgets of atmospheric glyoxal and methylglyoxal, and implications for formation of secondary organic aerosols. Journal of Geophysical Research, 2008, 113, .	3.3	575
9	NO _x emission trends for China, 1995–2004: The view from the ground and the view from space. Journal of Geophysical Research, 2007, 112, .	3.3	422
10	SCIAMACHY—scanning imaging absorption spectrometer for atmospheric chartography. Acta Astronautica, 1995, 35, 445-451.	1.7	403
11	ATMOSPHERIC REMOTE-SENSING REFERENCE DATA FROM GOME—2. TEMPERATURE-DEPENDENT ABSORPTION CROSS SECTIONS OF O3 IN THE 231–794NM RANGE. Journal of Quantitative Spectroscopy and Radiative Transfer, 1999, 61, 509-517.	1.1	397
12	Tropospheric NO2 from GOME measurements. Advances in Space Research, 2002, 29, 1673-1683.	1.2	361
13	Antarctic Springtime Depletion of Atmospheric Mercury. Environmental Science & Technology, 2002, 36, 1238-1244.	4.6	307
14	High spectral resolution ozone absorption cross-sections – Part 2: Temperature dependence. Atmospheric Measurement Techniques, 2014, 7, 625-636.	1.2	297
15	Global estimates of CO sources with high resolution by adjoint inversion of multiple satellite datasets (MOPITT, AIRS, SCIAMACHY, TES). Atmospheric Chemistry and Physics, 2010, 10, 855-876.	1.9	288
16	SCIATRAN 2.0 – A new radiative transfer model for geophysical applications in the 175–2400nm spectral region. Advances in Space Research, 2005, 36, 1015-1019.	1.2	281
17	Simultaneous global observations of glyoxal and formaldehyde from space. Geophysical Research Letters, 2006, 33, .	1.5	265
18	GOME observations of tropospheric BrO in northern hemispheric spring and summer 1997. Geophysical Research Letters, 1998, 25, 2683-2686.	1.5	264

#	Article	IF	CITATIONS
19	MAX-DOAS measurements of atmospheric trace gases in Ny-Ãlesund - Radiative transfer studies and their application. Atmospheric Chemistry and Physics, 2004, 4, 955-966.	1.9	251
20	Tropospheric Ozone Assessment Report: Present-day distribution and trends of tropospheric ozone relevant to climate and global atmospheric chemistry model evaluation. Elementa, 2018, 6, .	1.1	240
21	Megacities as hot spots of air pollution in the East Mediterranean. Atmospheric Environment, 2011, 45, 1223-1235.	1.9	239
22	Atmospheric methane and carbon dioxide from SCIAMACHY satellite data: initial comparison with chemistry and transport models. Atmospheric Chemistry and Physics, 2005, 5, 941-962.	1.9	238
23	Long-term changes of tropospheric NO ₂ over megacities derived from multiple satellite instruments. Atmospheric Chemistry and Physics, 2013, 13, 4145-4169.	1.9	237
24	Absorption cross-sections of NO2 in the UV and visible region (200 – 700 nm) at 298 K. Journal of Photochemistry and Photobiology A: Chemistry, 1987, 40, 195-217.	2.0	232
25	Radiative transfer through terrestrial atmosphere and ocean: Software package SCIATRAN. Journal of Quantitative Spectroscopy and Radiative Transfer, 2014, 133, 13-71.	1.1	225
26	Satellite-observed U.S. power plant NOxemission reductions and their impact on air quality. Geophysical Research Letters, 2006, 33, .	1.5	219
27	A remote sensing technique for global monitoring of power plant CO ₂ emissions from space and related applications. Atmospheric Measurement Techniques, 2010, 3, 781-811.	1.2	219
28	High-resolution absorption cross-section of glyoxal in the UV–vis and IR spectral ranges. Journal of Photochemistry and Photobiology A: Chemistry, 2005, 172, 35-46.	2.0	218
29	ATMOSPHERIC REMOTE-SENSING REFERENCE DATA FROM GOME: PART 1. TEMPERATURE-DEPENDENT ABSORPTION CROSS-SECTIONS OF NO2 IN THE 231–794 nm RANGE. Journal of Quantitative Spectroscopy and Radiative Transfer, 1998, 60, 1025-1031.	1.1	215
30	Frost flowers on sea ice as a source of sea salt and their influence on tropospheric halogen chemistry. Geophysical Research Letters, 2004, 31, .	1.5	202
31	New ultraviolet absorption cross-sections of BrO at atmospheric temperatures measured by time-windowing Fourier transform spectroscopy. Journal of Photochemistry and Photobiology A: Chemistry, 2004, 168, 117-132.	2.0	201
32	The temperature dependence (203–293 K) of the absorption cross sections of O3 in the 230–850 nm region measured by Fourier-transform spectroscopy. Journal of Photochemistry and Photobiology A: Chemistry, 2001, 143, 1-9.	2.0	196
33	RING EFFECT: IMPACT OF ROTATIONAL RAMAN SCATTERING ON RADIATIVE TRANSFER IN EARTH'S ATMOSPHERE. Journal of Quantitative Spectroscopy and Radiative Transfer, 1998, 60, 943-961.	1.1	195
34	A method for improved SCIAMACHY CO ₂ retrieval in the presence of optically thin clouds. Atmospheric Measurement Techniques, 2010, 3, 209-232.	1.2	194
35	The temperature and pressure dependence of the absorption cross-sections of NO2 in the 250–800 nm region measured by Fourier-transform spectroscopy. Journal of Photochemistry and Photobiology A: Chemistry, 2002, 149, 1-7.	2.0	186
36	MAX-DOAS measurements of formaldehyde in the Po-Valley. Atmospheric Chemistry and Physics, 2005, 5, 909-918.	1.9	184

#	Article	IF	CITATIONS
37	Tropospheric sulfur dioxide observed by the ERS-2 GOME instrument. Geophysical Research Letters, 1998, 25, 4177-4180.	1.5	178
38	The influence of natural and anthropogenic secondary sources on the glyoxal global distribution. Atmospheric Chemistry and Physics, 2008, 8, 4965-4981.	1.9	174
39	Peroxy radicals from night-time reaction of NO3 with organic compounds. Nature, 1990, 348, 147-149.	13.7	171
40	Comparison of box-air-mass-factors and radiances for Multiple-Axis Differential Optical Absorption Spectroscopy (MAX-DOAS) geometries calculated from different UV/visible radiative transfer models. Atmospheric Chemistry and Physics, 2007, 7, 1809-1833.	1.9	168
41	Carbon monoxide, methane and carbon dioxide columns retrieved from SCIAMACHY by WFM-DOAS: year 2003 initial data set. Atmospheric Chemistry and Physics, 2005, 5, 3313-3329.	1.9	162
42	A near-infrared optimized DOAS method for the fast global retrieval of atmospheric CH4, CO, CO2, H2O, and N2O total column amounts from SCIAMACHY Envisat-1 nadir radiances. Journal of Geophysical Research, 2000, 105, 15231-15245.	3.3	161
43	Long-term analysis of carbon dioxide and methane column-averaged mole fractions retrieved from SCIAMACHY. Atmospheric Chemistry and Physics, 2011, 11, 2863-2880.	1.9	158
44	Retrieval of atmospheric CO ₂ with enhanced accuracy and precision from SCIAMACHY: Validation with FTS measurements and comparison with model results. Journal of Geophysical Research, 2011, 116, .	3.3	153
45	Analysis for BrO in zenith-sky spectra: An intercomparison exercise for analysis improvement. Journal of Geophysical Research, 2002, 107, ACH 10-1.	3.3	152
46	Quantitative observation of cyanobacteria and diatoms from space using PhytoDOAS on SCIAMACHY data. Biogeosciences, 2009, 6, 751-764.	1.3	149
47	Space-based near-infrared CO2 measurements: Testing the Orbiting Carbon Observatory retrieval algorithm and validation concept using SCIAMACHY observations over Park Falls, Wisconsin. Journal of Geophysical Research, 2006, 111, .	3.3	146
48	Three years of greenhouse gas column-averaged dry air mole fractions retrieved from satellite – Part 1: Carbon dioxide. Atmospheric Chemistry and Physics, 2008, 8, 3827-3853.	1.9	146
49	NO ₂ columns in the western United States observed from space and simulated by a regional chemistry model and their implications for NO _x emissions. Journal of Geophysical Research, 2009, 114, .	3.3	146
50	The continental source of glyoxal estimated by the synergistic use of spaceborne measurements and inverse modelling. Atmospheric Chemistry and Physics, 2009, 9, 8431-8446.	1.9	146
51	High spectral resolution ozone absorption cross-sections – Part 1: Measurements, data analysis and comparison with previous measurements around 293 K. Atmospheric Measurement Techniques, 2014, 7, 609-624.	1.2	146
52	Satellite measurements of NO2from international shipping emissions. Geophysical Research Letters, 2004, 31, .	1.5	144
53	Ozone profiles from GOME satellite data: Algorithm description and first validation. Journal of Geophysical Research, 1999, 104, 8263-8280.	3.3	143
54	Atmospheric carbon gases retrieved from SCIAMACHY by WFM-DOAS: version 0.5 CO and CH ₄ and impact of calibration improvements on CO ₂ retrieval. Atmospheric Chemistry and Physics, 2006, 6, 2727-2751.	1.9	143

#	Article	IF	CITATIONS
55	Observations of iodine monoxide columns from satellite. Atmospheric Chemistry and Physics, 2008, 8, 637-653.	1.9	135
56	State of the Climate in 2010. Bulletin of the American Meteorological Society, 2011, 92, S1-S236.	1.7	135
57	GOMETRAN: A radiative transfer model for the satellite project GOME, the plane-parallel version. Journal of Geophysical Research, 1997, 102, 16683-16695.	3.3	134
58	Validation of ozone measurements from the Atmospheric Chemistry Experiment (ACE). Atmospheric Chemistry and Physics, 2009, 9, 287-343.	1.9	134
59	An improved NO ₂ retrieval for the GOME-2 satellite instrument. Atmospheric Measurement Techniques, 2011, 4, 1147-1159.	1.2	134
60	Ozone in the remote marine boundary layer: A possible role for halogens. Journal of Geophysical Research, 1999, 104, 21385-21395.	3.3	133
61	State of the Climate in 2012. Bulletin of the American Meteorological Society, 2013, 94, S1-S258.	1.7	129
62	Remote sensing of fugitive methane emissions from oil and gas production in North American tight geologic formations. Earth's Future, 2014, 2, 548-558.	2.4	129
63	Inverse modelling of the spatial distribution of NO _x emissions on a continental scale using satellite data. Atmospheric Chemistry and Physics, 2006, 6, 1747-1770.	1.9	127
64	Fire in the Air: Biomass Burning Impacts in a Changing Climate. Critical Reviews in Environmental Science and Technology, 2013, 43, 40-83.	6.6	125
65	Halogen oxides: Radicals, sources and reservoirs in the laboratory and in the atmosphere. Atmospheric Environment, 1995, 29, 2677-2881.	1.9	123
66	Systematic analysis of interannual and seasonal variations of model-simulated tropospheric NO ₂ in Asia and comparison with GOME-satellite data. Atmospheric Chemistry and Physics, 2007, 7, 1671-1681.	1.9	122
67	The Brewer-Dobson circulation and total ozone from seasonal to decadal time scales. Atmospheric Chemistry and Physics, 2011, 11, 11221-11235.	1.9	121
68	Tropospheric ozone over the tropical Atlantic: A satellite perspective. Journal of Geophysical Research, 2003, 108, .	3.3	119
69	Three years of greenhouse gas column-averaged dry air mole fractions retrieved from satellite – Part 2: Methane. Atmospheric Chemistry and Physics, 2009, 9, 443-465.	1.9	119
70	Total ozone trends from 1979 to 2016 derived from five merged observational datasets $\hat{a} \in $ the emergence into ozone recovery. Atmospheric Chemistry and Physics, 2018, 18, 2097-2117.	1.9	118
71	Total ozone retrieval from GOME UV spectral data using the weighting function DOAS approach. Atmospheric Chemistry and Physics, 2005, 5, 1015-1025.	1.9	114
72	GOME-2 observations of oxygenated VOCs: what can we learn from the ratio glyoxal to formaldehyde on a global scale?. Atmospheric Chemistry and Physics, 2010, 10, 10145-10160.	1.9	114

#	Article	lF	CITATIONS
73	The Greenhouse Gas Climate Change Initiative (GHG-CCI): Comparison and quality assessment of near-surface-sensitive satellite-derived CO2 and CH4 global data sets. Remote Sensing of Environment, 2015, 162, 344-362.	4.6	112
74	Gome measurements of stratospheric and tropospheric BrO. Advances in Space Research, 2002, 29, 1667-1672.	1.2	110
75	A study of the UV—visible absorption spectrum of molecular chlorine. Journal of Photochemistry and Photobiology A: Chemistry, 1993, 70, 205-214.	2.0	108
76	First direct observation of the atmospheric CO ₂ year-to-year increase from space. Atmospheric Chemistry and Physics, 2007, 7, 4249-4256.	1.9	108
77	Remote Sensing of Tropospheric Pollution from Space. Bulletin of the American Meteorological Society, 2008, 89, 805-822.	1.7	108
78	Temporal and spatial variability of glyoxal as observed from space. Atmospheric Chemistry and Physics, 2009, 9, 4485-4504.	1.9	108
79	Towards monitoring localized CO ₂ emissions from space: co-located regional CO ₂ and NO ₂ enhancements observed by the OCO-2 and S5P satellites. Atmospheric Chemistry and Physics. 2019. 19. 9371-9383.	1.9	107
80	A numerical radiative transfer model for a spherical planetary atmosphere: combined differential–integral approach involving the Picard iterative approximation. Journal of Quantitative Spectroscopy and Radiative Transfer, 2001, 69, 491-512.	1.1	106
81	On the possible causes of recent increases in northern hemispheric total ozone from a statistical analysis of satellite data from 1979 to 2003. Atmospheric Chemistry and Physics, 2006, 6, 1165-1180.	1.9	103
82	On the improvement of NO ₂ satellite retrievals – aerosol impact on the airmass factors. Atmospheric Measurement Techniques, 2010, 3, 475-493.	1.2	103
83	Kinetics and mechanism of the disproportionation of hydroperoxyl radical in the gas phase. The Journal of Physical Chemistry, 1979, 83, 2560-2568.	2.9	102
84	Sciatran - a new radiative transfer model for geophysical applications in the 240–2400 NM spectral region: the pseudo-spherical version. Advances in Space Research, 2002, 29, 1831-1835.	1.2	101
85	Decreasing emissions of NOx relative to CO2 in East Asia inferred from satellite observations. Nature Geoscience, 2014, 7, 792-795.	5.4	99
86	Evolution of stratospheric ozone and water vapour time series studied with satellite measurements. Atmospheric Chemistry and Physics, 2009, 9, 6055-6075.	1.9	98
87	Satellite measurements of atmospheric ozone profiles, including tropospheric ozone, from ultraviolet/visible measurements in the nadir geometry: a potential method to retrieve tropospheric ozone. Journal of Quantitative Spectroscopy and Radiative Transfer, 1997, 57, 467-476.	1.1	97
88	Global tropospheric NO2column distributions: Comparing three-dimensional model calculations with GOME measurements. Journal of Geophysical Research, 2001, 106, 12643-12660.	3.3	95
89	Validation of SCIAMACHY tropospheric NO ₂ -columns with AMAXDOAS measurements. Atmospheric Chemistry and Physics, 2005, 5, 1039-1051.	1.9	94
90	Ozone and temperature trends in the upper stratosphere at five stations of the Network for the Detection of Atmospheric Composition Change. International Journal of Remote Sensing, 2009, 30, 3875-3886.	1.3	94

#	Article	IF	CITATIONS
91	Carbon Monitoring Satellite (CarbonSat): assessment of atmospheric CO ₂ and CH ₄ retrieval errors by error parameterization. Atmospheric Measurement Techniques, 2013, 6, 3477-3500.	1.2	94
92	Total ozone during the unusual Antarctic winter of 2002. Geophysical Research Letters, 2003, 30, .	1.5	93
93	NO2 and BrO vertical profile retrieval from SCIAMACHY limb measurements: Sensitivity studies. Advances in Space Research, 2005, 36, 846-854.	1.2	93
94	Dynamical control of NH and SH winter/spring total ozone from GOME observations in 1995–2002. Geophysical Research Letters, 2003, 30, .	1.5	92
95	Carbonate precipitation in brine – a potential trigger for tropospheric ozone depletion events. Atmospheric Chemistry and Physics, 2006, 6, 4653-4658.	1.9	92
96	Ozone depletion during the solar proton events of October/November 2003 as seen by SCIAMACHY. Journal of Geophysical Research, 2005, 110, .	3.3	90
97	Analysis of global water vapour trends from satellite measurements in the visible spectral range. Atmospheric Chemistry and Physics, 2008, 8, 491-504.	1.9	90
98	Variations of the increasing trend of tropospheric NO2 over central east China during the past decade. Atmospheric Environment, 2007, 41, 4865-4876.	1.9	89
99	MAMAP – a new spectrometer system for column-averaged methane and carbon dioxide observations from aircraft: retrieval algorithm and first inversions for point source emission rates. Atmospheric Measurement Techniques, 2011, 4, 1735-1758.	1.2	89
100	Calibrated chemical amplifier for atmospheric ROx measurements. Analytical Chemistry, 1991, 63, 2048-2057.	3.2	88
101	A semianalytical cloud retrieval algorithm using backscattered radiation in 0.4–2.4 μm spectral region. Journal of Geophysical Research, 2003, 108, AAC 4-1.	3.3	88
102	Economic crisis detected from space: Air quality observations over Athens/Greece. Geophysical Research Letters, 2013, 40, 458-463.	1.5	88
103	MERLIN: A French-German Space Lidar Mission Dedicated to Atmospheric Methane. Remote Sensing, 2017, 9, 1052.	1.8	88
104	On the Cause of Recent Variations in Lower Stratospheric Ozone. Geophysical Research Letters, 2018, 45, 5718-5726.	1.5	87
105	Evidence of a natural marine source of oxalic acid and a possible link to glyoxal. Journal of Geophysical Research, 2011, 116, .	3.3	86
106	Atmospheric greenhouse gases retrieved from SCIAMACHY: comparison to ground-based FTS measurements and model results. Atmospheric Chemistry and Physics, 2012, 12, 1527-1540.	1.9	86
107	Evaluations of NO _x and highly reactive VOC emission inventories in Texas and their implications for ozone plume simulations during the Texas Air Quality Study 2006. Atmospheric Chemistry and Physics, 2011, 11, 11361-11386.	1.9	85
108	Trend analysis of aerosol optical thickness and Ångström exponent derived from the global AERONET spectral observations. Atmospheric Measurement Techniques, 2012, 5, 1271-1299.	1.2	85

#	Article	IF	CITATIONS
109	Global carbon monoxide as retrieved from SCIAMACHY by WFM-DOAS. Atmospheric Chemistry and Physics, 2004, 4, 1945-1960.	1.9	84
110	Three years of global carbon monoxide from SCIAMACHY: comparison with MOPITT and first results related to the detection of enhanced CO over cities. Atmospheric Chemistry and Physics, 2007, 7, 2399-2411.	1.9	84
111	Satellite measurement based estimates of decadal changes in European nitrogen oxides emissions. Atmospheric Chemistry and Physics, 2008, 8, 2623-2641.	1.9	84
112	First retrieval of global water vapour column amounts from SCIAMACHY measurements. Atmospheric Chemistry and Physics, 2004, 4, 111-125.	1.9	83
113	Satellite-inferred European carbon sink larger than expected. Atmospheric Chemistry and Physics, 2014, 14, 13739-13753.	1.9	83
114	Analysis of tropospheric NOx over Asia using the model of atmospheric transport and chemistry (MATCH-MPIC) and GOME-satellite observations. Atmospheric Environment, 2004, 38, 581-596.	1.9	82
115	Satellite measurements of daily variations in soil NOxemissions. Geophysical Research Letters, 2005, 32, .	1.5	82
116	Exploring the missing source of glyoxal (CHOCHO) over China. Geophysical Research Letters, 2012, 39, .	1.5	82
117	Intercomparison of BrO measurements from ERS-2 GOME, ground-based and balloon platforms. Advances in Space Research, 2002, 29, 1661-1666.	1.2	80
118	Spectroscopic studies of the I2/O3 photochemistry. Journal of Photochemistry and Photobiology A: Chemistry, 2005, 176, 50-67.	2.0	79
119	Global observations of stratospheric bromine monoxide from SCIAMACHY. Geophysical Research Letters, 2005, 32, .	1.5	79
120	Total ozone trends and variability during 1979–2012 from merged data sets of various satellites. Atmospheric Chemistry and Physics, 2014, 14, 7059-7074.	1.9	79
121	Intercomparison of oxygenated volatile organic compound measurements at the SAPHIR atmosphere simulation chamber. Journal of Geophysical Research, 2008, 113, .	3.3	78
122	MAMAP – a new spectrometer system for column-averaged methane and carbon dioxide observations from aircraft: instrument description and performance analysis. Atmospheric Measurement Techniques, 2011, 4, 215-243.	1.2	78
123	Formaldehyde and nitrogen dioxide over the remote western Pacific Ocean: SCIAMACHY and GOME-2 validation using ship-based MAX-DOAS observations. Atmospheric Chemistry and Physics, 2012, 12, 11179-11197.	1.9	76
124	SCIAMACHY formaldehyde observations: constraint for isoprene emission estimates over Europe?. Atmospheric Chemistry and Physics, 2009, 9, 1647-1664.	1.9	74
125	Remote sensing of methane leakage from natural gas and petroleum systems revisited. Atmospheric Chemistry and Physics, 2020, 20, 9169-9182.	1.9	74
126	Large loss of total ozone during the Arctic winter of 1999/2000. Geophysical Research Letters, 2000, 27, 3473-3476.	1.5	73

#	Article	IF	CITATIONS
127	Anthropogenic carbon dioxide source areas observed from space: assessment of regional enhancements and trends. Atmospheric Chemistry and Physics, 2013, 13, 2445-2454.	1.9	73
128	Changes in atmospheric aerosol loading retrieved from space-based measurements during the past decade. Atmospheric Chemistry and Physics, 2014, 14, 6881-6902.	1.9	72
129	Retrieval of atmospheric constituents in the uv-visible: a new quasi-analytical approach for the calculation of weighting functions. Journal of Quantitative Spectroscopy and Radiative Transfer, 1998, 60, 277-299.	1.1	71
130	Atmospheric water vapor amounts retrieved from GOME satellite data. Geophysical Research Letters, 1999, 26, 1841-1844.	1.5	71
131	Pole-to-pole validation of GOME WFDOAS total ozone with groundbased data. Atmospheric Chemistry and Physics, 2005, 5, 1341-1355.	1.9	71
132	A scientific algorithm to simultaneously retrieve carbon monoxide and methane from TROPOMI onboard Sentinel-5 Precursor. Atmospheric Measurement Techniques, 2019, 12, 6771-6802.	1.2	71
133	Satellite observations of long range transport of a large BrO plume in the Arctic. Atmospheric Chemistry and Physics, 2010, 10, 6515-6526.	1.9	70
134	The Greenhouse Gas Climate Change Initiative (GHG-CCI): comparative validation of GHG-CCI SCIAMACHY/ENVISAT and TANSO-FTS/GOSAT CO ₂ and CH ₄ retrieval algorithm products with measurements from the TCCON. Atmospheric Measurement Techniques, 2014, 7, 1723-1744.	1.2	70
135	A study of the UV—visible absorption spectra of Br2 and BrCl. Journal of Photochemistry and Photobiology A: Chemistry, 1994, 83, 179-192.	2.0	69
136	Kinetics and mechanism of the photooxidation of formaldehyde. 2. Molecular modulation studies. The Journal of Physical Chemistry, 1989, 93, 2375-2382.	2.9	68
137	BrO emission from volcanoes: A survey using GOME and SCIAMACHY measurements. Geophysical Research Letters, 2004, 31, .	1.5	68
138	Multi-annual changes of NO _x emissions in megacity regions: nonlinear trend analysis of satellite measurement based estimates. Atmospheric Chemistry and Physics, 2010, 10, 8481-8498.	1.9	68
139	Investigation of NO _x emissions and NO _x -related chemistry in East Asia using CMAQ-predicted and GOME-derived NO ₂ columns. Atmospheric Chemistry and Physics, 2009, 9, 1017-1036.	1.9	67
140	On the dependence of the OH [*] Meinel emission altitude on vibrational level: SCIAMACHY observations and model simulations. Atmospheric Chemistry and Physics, 2012, 12, 8813-8828.	1.9	67
141	Quantification of methane emission rates from coal mine ventilation shafts using airborne remote sensing data. Atmospheric Measurement Techniques, 2013, 6, 151-166.	1.2	67
142	Peroxy radical and related trace gas measurements in the boundary layer above the Atlantic Ocean. Journal of Geophysical Research, 2001, 106, 5457-5477.	3.3	66
143	The Ozone Hole Breakup in September 2002 as Seen by SCIAMACHY on ENVISAT. Journals of the Atmospheric Sciences, 2005, 62, 721-734.	0.6	66
144	Measurements of nitrogen dioxide total column amounts using a Brewer double spectrophotometer in direct Sun mode. Journal of Geophysical Research, 2006, 111, .	3.3	66

#	Article	IF	CITATIONS
145	SO ₂ Retrieval from SCIAMACHY using the Weighting Function DOAS (WFDOAS) technique: comparison with Standard DOAS retrieval. Atmospheric Chemistry and Physics, 2008, 8, 6137-6145.	1.9	66
146	Stratospheric ozone trends and variability as seen by SCIAMACHY from 2002 to 2012. Atmospheric Chemistry and Physics, 2014, 14, 831-846.	1.9	66
147	Comparison of model-simulated tropospheric NO2 over China with GOME-satellite data. Atmospheric Environment, 2006, 40, 593-604.	1.9	65
148	A global stratospheric bromine monoxide climatology based on the BASCOE chemical transport model. Atmospheric Chemistry and Physics, 2009, 9, 831-848.	1.9	65
149	Validation of NO ₂ and NO from the Atmospheric Chemistry Experiment (ACE). Atmospheric Chemistry and Physics, 2008, 8, 5801-5841.	1.9	64
150	Title is missing!. Journal of Atmospheric Chemistry, 1999, 32, 281-314.	1.4	63
151	Evaluation of long-term tropospheric NO2data obtained by GOME over East Asia in 1996–2002. Geophysical Research Letters, 2005, 32, .	1.5	63
152	Satellite-derived methane hotspot emission estimates using a fast data-driven method. Atmospheric Chemistry and Physics, 2017, 17, 5751-5774.	1.9	63
153	Comparison of measurements and model calculations of stratospheric bromine monoxide. Journal of Geophysical Research, 2002, 107, ACH 11-1.	3.3	62
154	Rapid intercontinental air pollution transport associated with a meteorological bomb. Atmospheric Chemistry and Physics, 2003, 3, 969-985.	1.9	62
155	Comparison of 7 years of satellite-borne and ground-based tropospheric NO2measurements around Milan, Italy. Journal of Geophysical Research, 2006, 111, .	3.3	62
156	Kinetic and Mechanistic Studies of the I2/O3 Photochemistry. Journal of Physical Chemistry A, 2007, 111, 306-320.	1.1	62
157	A joint effort to deliver satellite retrieved atmospheric CO ₂ concentrations for surface flux inversions: the ensemble median algorithm EMMA. Atmospheric Chemistry and Physics, 2013, 13, 1771-1780.	1.9	62
158	Comparison of satellite observed tropospheric NO2 over India with model simulations. Atmospheric Environment, 2010, 44, 3314-3321.	1.9	61
159	Rates of reaction of HO2 with HO and O studied by laser magnetic resonance. Nature, 1977, 267, 233-234.	13.7	60
160	CO ₂ emission of Indonesian fires in 2015 estimated from satelliteâ€derived atmospheric CO ₂ concentrations. Geophysical Research Letters, 2017, 44, 1537-1544.	1.5	60
161	First observation of the OIO molecule by time-resolved flash photolysis absorption spectroscopy. Chemical Physics Letters, 1996, 251, 330-334.	1.2	59
162	A correlated-kdistribution scheme for overlapping gases suitable for retrieval of atmospheric constituents from moderate resolution radiance measurements in the visible/near-infrared spectral region. Journal of Geophysical Research, 2000, 105, 15247-15261.	3.3	59

#	Article	IF	CITATIONS
163	Measurements of iodine monoxide (IO) above Spitsbergen. Geophysical Research Letters, 2000, 27, 1471-1474.	1.5	59
164	Comparison of total ozone from the satellite instruments GOME and TOMS with measurements from the Dobson network 1996–2000. Atmospheric Chemistry and Physics, 2003, 3, 1409-1419.	1.9	59
165	Retrieval of spectral aerosol optical thickness over land using ocean color sensors MERIS and SeaWiFS. Atmospheric Measurement Techniques, 2011, 4, 151-171.	1.2	59
166	Monitoring compliance with sulfur content regulations of shipping fuel by in situ measurements of ship emissions. Atmospheric Chemistry and Physics, 2015, 15, 10087-10092.	1.9	59
167	On the isomerisation of the methoxy radical relevance to atmospheric chemistry and combustion. Chemical Physics Letters, 1981, 78, 467-470.	1.2	58
168	Combined differential-integral approach for the radiation field computation in a spherical shell atmosphere: Nonlimb geometry. Journal of Geophysical Research, 2000, 105, 22937-22942.	3.3	58
169	The relationship between tropospheric wave forcing and tropical lower stratospheric water vapor. Atmospheric Chemistry and Physics, 2008, 8, 471-480.	1.9	58
170	Towards space based verification of CO ₂ emissions from strong localized sources: fossil fuel power plant emissions as seen by a CarbonSat constellation. Atmospheric Measurement Techniques, 2011, 4, 2809-2822.	1.2	58
171	Ozone profile retrieval from Global Ozone Monitoring Experiment (GOME) data using a neural network approach (Neural Network Ozone Retrieval System (NNORSY)). Journal of Geophysical Research, 2003, 108, .	3.3	57
172	Spatial and temporal characterization of SCIAMACHY limb pointing errors during the first three years of the mission. Atmospheric Chemistry and Physics, 2005, 5, 2593-2602.	1.9	57
173	Influence of low spatial resolution a priori data on tropospheric NO ₂ satellite retrievals. Atmospheric Measurement Techniques, 2011, 4, 1805-1820.	1.2	57
174	Observation of a fast ozone loss in the marginal ice zone of the Arctic Ocean. Journal of Geophysical Research, 2006, 111, .	3.3	56
175	Retrieval of aerosol optical properties using MERIS observations: Algorithm and some first results. Remote Sensing of Environment, 2017, 197, 125-140.	4.6	56
176	A model study of the impact of magnetic field structure on atmospheric composition during solar proton events. Geophysical Research Letters, 2003, 30, .	1.5	55
177	Lightweight diode laser spectrometer CHILD (Compact High-altitude In-situ Laser Diode) for balloonborne measurements of water vapor and methane. Applied Optics, 2005, 44, 91.	2.1	55
178	Forest fire plumes over the North Atlantic: p-TOMCAT model simulations with aircraft and satellite measurements from the ITOP/ICARTT campaign. Journal of Geophysical Research, 2007, 112, .	3.3	55
179	Terrestrial carbon sink observed from space: variation of growth rates and seasonal cycle amplitudes in response to interannual surface temperature variability. Atmospheric Chemistry and Physics, 2014, 14, 133-141.	1.9	55
180	Atmospheric Reactions of the HOFormula Radical Studied by Laser Magnetic Resonance Spectroscopy. Proceedings of the Royal Society A: Mathematical, Physical and Engineering Sciences, 1979, 368, 463-481.	1.0	54

#	Article	IF	CITATIONS
181	Inelastic scattering in ocean water and its impact on trace gas retrievals from satellite data. Atmospheric Chemistry and Physics, 2003, 3, 1365-1375.	1.9	54
182	Vertical variation of NLC particle sizes retrieved from Odin/OSIRIS limb scattering observations. Geophysical Research Letters, 2005, 32, n/a-n/a.	1.5	54
183	Regional NOx emission inversion through a four-dimensional variational approach using SCIAMACHY tropospheric NO2 column observations. Atmospheric Environment, 2009, 43, 5046-5055.	1.9	54
184	Analysis of linear long-term trend of aerosol optical thickness derived from SeaWiFS using BAER over Europe and South China. Atmospheric Chemistry and Physics, 2011, 11, 12149-12167.	1.9	54
185	First comparison of tropospheric NO2column densities retrieved from GOME measurements and in situ aircraft profile measurements. Geophysical Research Letters, 2002, 29, 44-1-44-4.	1.5	53
186	On the disappearance of noctilucent clouds during the January 2005 solar proton events. Geophysical Research Letters, 2007, 34, .	1.5	53
187	Impact of forest fires, biogenic emissions and high temperatures on the elevated Eastern Mediterranean ozone levels during the hot summer of 2007. Atmospheric Chemistry and Physics, 2012, 12, 8727-8750.	1.9	52
188	Global satellite observations of column-averaged carbon dioxide and methane: The GHG-CCI XCO2 and XCH4 CRDP3 data set. Remote Sensing of Environment, 2017, 203, 276-295.	4.6	52
189	The ring effect in the cloudy atmosphere. Geophysical Research Letters, 2001, 28, 721-724.	1.5	51
190	Simultaneous satellite observations of IO and BrO over Antarctica. Atmospheric Chemistry and Physics, 2012, 12, 6565-6580.	1.9	51
191	Global retrieval of marine and terrestrial chlorophyll fluorescence at its red peak using hyperspectral top of atmosphere radiance measurements: Feasibility study and first results. Remote Sensing of Environment, 2015, 166, 243-261.	4.6	51
192	Tracking city CO ₂ emissions from space using a high-resolution inverse modelling approach: a case study for Berlin, Germany. Atmospheric Chemistry and Physics, 2016, 16, 9591-9610.	1.9	51
193	New measurements of OClO absorption cross-sections in the 325–435 nm region and their temperature dependence between 213 and 293 K. Journal of Photochemistry and Photobiology A: Chemistry, 2003, 157, 149-160.	2.0	50
194	Impact of the 2009 Attica wild fires on the air quality in urban Athens. Atmospheric Environment, 2012, 46, 536-544.	1.9	50
195	SCIAMACHY solar irradiance observation in the spectral range from 240 to 2380nm. Advances in Space Research, 2005, 35, 370-375.	1.2	48
196	Integrated water vapor above Ny Ã…lesund, Spitsbergen: a multi-sensor intercomparison. Atmospheric Chemistry and Physics, 2010, 10, 1215-1226.	1.9	48
197	Investigation of the effect of water complexes in the determination of peroxy radical ambient concentrations: Implications for the atmosphere. Journal of Geophysical Research, 2003, 108, ACH 4-1.	3.3	47
198	Ozone column classified climatology of ozone and temperature profiles based on ozonesonde and satellite data. Journal of Geophysical Research, 2004, 109, .	3.3	47

#	Article	IF	CITATIONS
199	Global satellite validation of SCIAMACHY O ₃ columns with GOME WFDOAS. Atmospheric Chemistry and Physics, 2005, 5, 2357-2368.	1.9	47
200	Ship emitted NO ₂ in the Indian Ocean: comparison of model results with satellite data. Atmospheric Chemistry and Physics, 2009, 9, 7289-7301.	1.9	47
201	Unexpected long-range transport of glyoxal and formaldehyde observed from the Copernicus Sentinel-5 Precursor satellite during the 2018 Canadian wildfires. Atmospheric Chemistry and Physics, 2020, 20, 2057-2072.	1.9	47
202	Peroxy radical reactions in the photo-oxidation of CH3CHO. Journal of the Chemical Society, Faraday Transactions 2, 1989, 85, 809.	1.1	46
203	Comparison and evaluation of modelled and GOME measurement derived tropospheric NO ₂ columns over Western and Eastern Europe. Atmospheric Chemistry and Physics, 2005, 5, 169-190.	1.9	46
204	Preliminary results of GOME-2 water vapour retrievals and first applications in polar regions. Atmospheric Chemistry and Physics, 2008, 8, 1519-1529.	1.9	46
205	Title is missing!. Solar Physics, 1998, 177, 63-77.	1.0	45
206	Using GOME NO ₂ satellite data to examine regional differences in TOMCAT model performance. Atmospheric Chemistry and Physics, 2004, 4, 1895-1912.	1.9	45
207	Spectroscopic studies of the I2/O3 photochemistry. Journal of Photochemistry and Photobiology A: Chemistry, 2005, 176, 15-38.	2.0	45
208	Satellite observations of the quasi 5â€day wave in noctilucent clouds and mesopause temperatures. Geophysical Research Letters, 2007, 34, .	1.5	45
209	BrO vertical distributions from SCIAMACHY limb measurements: comparison of algorithms and retrieval results. Atmospheric Measurement Techniques, 2011, 4, 1319-1359.	1.2	45
210	Consistent satellite XCO ₂ retrievals from SCIAMACHY and GOSAT using the BESD algorithm. Atmospheric Measurement Techniques, 2015, 8, 2961-2980.	1.2	45
211	Absorption spectrum of NO3 and kinetics of the reactions of NO3 with NO2, Cl, and several stable atmospheric species at 298 K. The Journal of Physical Chemistry, 1985, 89, 4848-4856.	2.9	44
212	Application of a Gaussian Distribution Function To Describe Molecular UVâ^Visible Absorption Continua. 1. Theory. The Journal of Physical Chemistry, 1996, 100, 8645-8659.	2.9	44
213	Global distribution of atmospheric bromine-monoxide from GOME on Earth Observing Satellite ERS-2. Geophysical Research Letters, 1998, 25, 3127-3130.	1.5	44
214	DOAS Zenith Sky Observations: 2. Seasonal Variation of BrO Over Bremen (53°N) 1994-1995. Journal of Atmospheric Chemistry, 1999, 32, 83-99.	1.4	44
215	Satellite-pointing retrieval from atmospheric limb-scattering of solar UV-B radiation. Canadian Journal of Physics, 2004, 82, 1041-1052.	0.4	44
216	Global distribution pattern of anthropogenic nitrogen oxide emissions: Correlation analysis of satellite measurements and model calculations. Journal of Geophysical Research, 2006, 111, .	3.3	44

#	Article	IF	CITATIONS
217	Simultaneous determination of aerosol- and surface characteristics from top-of-atmosphere reflectance using MERIS on board of ENVISAT. Advances in Space Research, 2006, 37, 2172-2177.	1.2	44
218	Measurements of tropospheric NO ₂ with an airborne multi-axis DOAS instrument. Atmospheric Chemistry and Physics, 2005, 5, 337-343.	1.9	43
219	Field and satellite observations of the formation and distribution of Arctic atmospheric bromine above a rejuvenated sea ice cover. Journal of Geophysical Research, 2012, 117, .	3.3	43
220	Tropospheric NO ₂ columns: a comparison between model and retrieved data from GOME measurements. Atmospheric Chemistry and Physics, 2002, 2, 67-78.	1.9	42
221	NLC detection and particle size determination: first results from SCIAMACHY on ENVISAT. Advances in Space Research, 2004, 34, 851-856.	1.2	42
222	First near-global retrievals of OH rotational temperatures from satellite-based Meinel band emission measurements. Geophysical Research Letters, 2004, 31, .	1.5	42
223	Validation of SCIAMACHY AMC-DOAS water vapour columns. Atmospheric Chemistry and Physics, 2005, 5, 1835-1841.	1.9	42
224	Cloud sensitivity studies for stratospheric and lower mesospheric ozone profile retrievals from measurements of limb-scattered solar radiation. Atmospheric Measurement Techniques, 2009, 2, 653-678.	1.2	42
225	An improved glyoxal retrieval from OMI measurements. Atmospheric Measurement Techniques, 2014, 7, 4133-4150.	1.2	42
226	A Cloud masking algorithm for the XBAER aerosol retrieval using MERIS data. Remote Sensing of Environment, 2017, 197, 141-160.	4.6	42
227	OCS formation in the reaction of OH with CS2. Chemical Physics Letters, 1982, 88, 372-376.	1.2	41
228	SOLAR VARIABILITY FROM 240 TO 1750 nm IN TERMS OF FACULAE BRIGHTENING AND SUNSPOT DARKENING FROM SCIAMACHY. Astrophysical Journal, 2009, 700, 1884-1895.	1.6	41
229	Very high ozone columns at northern mid-latitudes in 2010. Geophysical Research Letters, 2011, 38, n/a-n/a.	1.5	41
230	Enhanced O3and NO2in thunderstorm clouds: Convection or production?. Geophysical Research Letters, 1999, 26, 1291-1294.	1.5	40
231	Detection and mapping of polar stratospheric clouds using limb scattering observations. Atmospheric Chemistry and Physics, 2005, 5, 3071-3079.	1.9	40
232	Airborne multi-axis DOAS measurements of tropospheric SO ₂ plumes in the Po-valley, Italy. Atmospheric Chemistry and Physics, 2006, 6, 329-338.	1.9	40
233	Using a photochemical model for the validation of NO ₂ satellite measurements at different solar zenith angles. Atmospheric Chemistry and Physics, 2005, 5, 393-408.	1.9	39
234	The detection of cloud-free snow-covered areas using AATSR measurements. Atmospheric Measurement Techniques, 2010, 3, 1005-1017.	1.2	39

#	Article	lF	CITATIONS
235	GOME Observations of Stratospheric Trace Gas Distributions during the Splitting Vortex Event in the Antarctic Winter of 2002. Part I: Measurements. Journals of the Atmospheric Sciences, 2005, 62, 778-785.	0.6	38
236	Impact of transport of sulfur dioxide from the Asian continent on the air quality over Korea during May 2005. Atmospheric Environment, 2008, 42, 1461-1475.	1.9	38
237	Glyoxal observations in the global marine boundary layer. Journal of Geophysical Research D: Atmospheres, 2014, 119, 6160-6169.	1.2	38
238	Ability of the 4-D-Var analysis of the GOSAT BESD XCO ₂ retrievals to characterize atmospheric CO ₂ at large and synoptic scales. Atmospheric Chemistry and Physics, 2016, 16, 1653-1671.	1.9	38
239	Enhanced trans-Himalaya pollution transport to the Tibetan Plateau by cut-off low systems. Atmospheric Chemistry and Physics, 2017, 17, 3083-3095.	1.9	38
240	Distribution of volatile organic compounds over Indian subcontinent during winter: WRF-chem simulation versus observations. Environmental Pollution, 2019, 252, 256-269.	3.7	38
241	Retrieval of CH 4 , CO, and CO 2 total column amounts from SCIAMACHY near-infrared nadir spectra: retrieval algorithm and first results. , 2004, , .		37
242	Atmospheric aerosol load as derived from space. Atmospheric Research, 2006, 81, 176-185.	1.8	37
243	Tropospheric column amount of ozone retrieved from SCIAMACHY limb–nadir-matching observations. Atmospheric Measurement Techniques, 2014, 7, 2073-2096.	1.2	37
244	The empirical relationship between satellite-derived tropospheric NO ₂ and fire radiative power and possible implications for fire emission rates of NO _x . Atmospheric Chemistry and Physics, 2014, 14, 2447-2466.	1.9	37
245	Measurements of line strengths in the hydroperoxy .nu.1 overtone band at 1.5 .mu.m using an indium gallium arsenide phosphide laser. The Journal of Physical Chemistry, 1991, 95, 6499-6502.	2.9	36
246	Stratospheric and tropospheric NO ₂ variability on the diurnal and annual scale: a combined retrieval from ENVISAT/SCIAMACHY and solar FTIR at the Permanent Ground-Truthing Facility Zugspitze/Garmisch. Atmospheric Chemistry and Physics, 2005, 5, 2657-2677.	1.9	36
247	Spectral studies of ocean water with space-borne sensor SCIAMACHY using Differential Optical Absorption Spectroscopy (DOAS). Ocean Science, 2007, 3, 429-440.	1.3	36
248	Satellite measurements of formaldehyde linked to shipping emissions. Atmospheric Chemistry and Physics, 2009, 9, 8223-8234.	1.9	36
249	First evidence of a 27 day solar signature in noctilucent cloud occurrence frequency. Journal of Geophysical Research, 2010, 115, .	3.3	36
250	Odin/OSIRIS observations of stratospheric BrO: Retrieval methodology, climatology, and inferred Br _{<i>y</i>} . Journal of Geophysical Research, 2010, 115, .	3.3	36
251	Aerosol optical depth retrieval in the Arctic region using MODIS data over snow. Remote Sensing of Environment, 2013, 128, 234-245.	4.6	36
252	Global investigation of the Mg atom and ion layers using SCIAMACHY/Envisat observations between 70 and 150 km altitude and WACCM-Mg model results. Atmospheric Chemistry and Physics, 2015, 15, 273-295.	1.9	36

#	Article	IF	CITATIONS
253	Ship-based MAX-DOAS measurements of tropospheric NO 2 and SO 2 in the South China and Sulu Sea. Atmospheric Environment, 2015, 102, 331-343.	1.9	36
254	Methane emissions from aÂCalifornian landfill, determined from airborne remote sensing and in situ measurements. Atmospheric Measurement Techniques, 2017, 10, 3429-3452.	1.2	36
255	Frequency modulation spectroscopy at 13 μm using InGaAsP lasers: a prototype field instrument for atmospheric chemistry research. Applied Optics, 1991, 30, 407.	2.1	35
256	Vibrational progressions in the visible and near-ultraviolet absorption spectrum of ozone. Chemical Physics Letters, 2001, 349, 241-248.	1.2	35
257	NO ₂ Profile retrieval using airborne multi axis UV-visible skylight absorption measurements over central Europe. Atmospheric Chemistry and Physics, 2006, 6, 3049-3058.	1.9	35
258	Comparison of the inversion algorithms applied to the ozone vertical profile retrieval from SCIAMACHY limb measurements. Atmospheric Chemistry and Physics, 2007, 7, 4763-4779.	1.9	35
259	Observation and integrated Earth-system science: A roadmap for 2016–2025. Advances in Space Research, 2016, 57, 2037-2103.	1.2	35
260	Cross comparisons of O3 and NO2 measured by the atmospheric ENVISAT instruments GOMOS, MIPAS, and SCIAMACHY. Advances in Space Research, 2005, 36, 855-867.	1.2	34
261	Regional NOxemission strength for the Indian subcontinent and the impact of emissions from India and neighboring countries on regional O3chemistry. Journal of Geophysical Research, 2006, 111, .	3.3	34
262	Improvements to the retrieval of tropospheric NO ₂ from satellite – stratospheric correction using SCIAMACHY limb/nadir matching and comparison to Oslo CTM2 simulations. Atmospheric Measurement Techniques, 2013, 6, 565-584.	1.2	34
263	Global tropospheric ozone variations from 2003 to 2011 as seen by SCIAMACHY. Atmospheric Chemistry and Physics, 2016, 16, 417-436.	1.9	34
264	Arctic Ozone Depletion in 2019/20: Roles of Chemistry, Dynamics and the Montreal Protocol. Geophysical Research Letters, 2021, 48, e2020GL091911.	1.5	34
265	Kinetics of chlorine oxide radical reactions using modulated photolysis. Part 4.—The reactions Cl + Cl2O → Cl2+ ClO and ClO + HO2→ products studied at 1 atm and 300c k. Journal of the Chemical Society Faraday Transactions I, 1981, 77, 2465.	1.0	33
266	Retrieval of profile information from airborne multiaxis UV-visible skylight absorption measurements. Applied Optics, 2004, 43, 4415.	2.1	33
267	Impact of ship emissions on the microphysical, optical and radiative properties of marine stratus: a case study. Atmospheric Chemistry and Physics, 2006, 6, 4925-4942.	1.9	33
268	Climatology of noctilucent cloud radii and occurrence frequency using SCIAMACHY. Journal of Atmospheric and Solar-Terrestrial Physics, 2009, 71, 408-423.	0.6	33
269	Remote sensing of aerosols over snow using infrared AATSR observations. Atmospheric Measurement Techniques, 2011, 4, 1133-1145.	1.2	33
270	Linear trends in cloud top height from passive observations in the oxygen A-band. Atmospheric Chemistry and Physics, 2014, 14, 5679-5692.	1.9	33

#	Article	IF	CITATIONS
271	How Much CO2 Is Taken Up by the European Terrestrial Biosphere?. Bulletin of the American Meteorological Society, 2017, 98, 665-671.	1.7	33
272	Study of the reaction chlorine monoxide + methyl peroxide .fwdarw. products at 300 K. The Journal of Physical Chemistry, 1989, 93, 7807-7813.	2.9	32
273	The determination of cloud altitudes using GOME reflectance spectra: multilayered cloud systems. IEEE Transactions on Geoscience and Remote Sensing, 2004, 42, 1009-1017.	2.7	32
274	The SCIAMACHY cloud products: Algorithms and examples from ENVISAT. Advances in Space Research, 2005, 36, 789-799.	1.2	32
275	A longâ€ŧerm stratospheric ozone data set from assimilation of satellite observations: Highâ€ŀatitude ozone anomalies. Journal of Geophysical Research, 2010, 115, .	3.3	32
276	Retrieval of water vapor vertical distributions in the upper troposphere and the lower stratosphere from SCIAMACHY limb measurements. Atmospheric Measurement Techniques, 2011, 4, 933-954.	1.2	32
277	Retrieval of aerosol optical depth over land surfaces from AVHRR data. Atmospheric Measurement Techniques, 2014, 7, 2411-2420.	1.2	32
278	Particles and iodine compounds in coastal Antarctica. Journal of Geophysical Research D: Atmospheres, 2015, 120, 7144-7156.	1.2	32
279	Slant column MAX-DOAS measurements of nitrogen dioxide, formaldehyde, glyoxal and oxygen dimer in the urban environment of Athens. Atmospheric Environment, 2016, 135, 118-131.	1.9	32
280	Kinetics of the reaction of OH with ClO. Journal of the Chemical Society, Faraday Transactions 2, 1984, 80, 957.	1.1	31
281	A study of the CIO absorption cross-section between 240 and 310 nm and the kinetics of the self-reaction at 300 K. Journal of Photochemistry and Photobiology A: Chemistry, 1990, 55, 1-23.	2.0	31
282	Tunable diode laser measurements of trace gases during the 1988 Polarstern cruise and intercomparisons with other methods. Journal of Atmospheric Chemistry, 1992, 15, 315-326.	1.4	31
283	Marine boundary layer peroxy radical chemistry during the AEROSOLS99 campaign: Measurements and analysis. Journal of Geophysical Research, 2001, 106, 20833-20846.	3.3	31
284	A study of the trace gas columns of O3, NO2 and HCHO over Africa in September 1997. Faraday Discussions, 2005, 130, 387.	1.6	31
285	Validation of SCIAMACHY top-of-atmosphere reflectance for aerosol remote sensing using MERIS L1 data. Atmospheric Chemistry and Physics, 2007, 7, 97-106.	1.9	31
286	Peroxy radical observations over West Africa during AMMA 2006: photochemical activity in the outflow of convective systems. Atmospheric Chemistry and Physics, 2009, 9, 3681-3695.	1.9	31
287	Attribution of stratospheric ozone trends to chemistry and transport: a modelling study. Atmospheric Chemistry and Physics, 2010, 10, 12073-12089.	1.9	31
288	Seven years of global retrieval of cloud properties using space-borne data of GOME. Atmospheric Measurement Techniques, 2012, 5, 1551-1570.	1.2	31

#	Article	IF	CITATIONS
289	Traveling planetary wave activity from mesopause region airglow temperatures determined by the Network for the Detection of Mesospheric Change (NDMC). Journal of Atmospheric and Solar-Terrestrial Physics, 2014, 119, 71-82.	0.6	31
290	Monitoring shipping emissions in the German Bight using MAX-DOAS measurements. Atmospheric Chemistry and Physics, 2017, 17, 10997-11023.	1.9	31
291	Retrieval of ozone profiles from OMPS limb scattering observations. Atmospheric Measurement Techniques, 2018, 11, 2135-2149.	1.2	31
292	Modeling the Sources and Chemistry of Polar Tropospheric Halogens (Cl, Br, and I) Using the CAM hem Global Chemistry limate Model. Journal of Advances in Modeling Earth Systems, 2019, 11, 2259-2289.	1.3	31
293	Parameterization schemes for terrestrial water clouds in the radiative transfer model GOMETRAN. Journal of Geophysical Research, 1997, 102, 21809-21823.	3.3	30
294	The semianalytical cloud retrieval algorithm for SCIAMACHY I. The validation. Atmospheric Chemistry and Physics, 2006, 6, 1905-1911.	1.9	30
295	A wide field-of-view imaging DOAS instrument for two-dimensional trace gas mapping from aircraft. Atmospheric Measurement Techniques, 2015, 8, 5113-5131.	1.2	30
296	Clobal and long-term comparison of SCIAMACHY limb ozone profiles with correlative satellite data (2002–2008). Atmospheric Measurement Techniques, 2012, 5, 771-788.	1.2	29
297	A simple empirical model estimating atmospheric CO ₂ background concentrations. Atmospheric Measurement Techniques, 2012, 5, 1349-1357.	1.2	29
298	Comparison of the HadGEM2 climate-chemistry model against in situ and SCIAMACHY atmospheric methane data. Atmospheric Chemistry and Physics, 2014, 14, 13257-13280.	1.9	29
299	Chemical ozone loss and ozone mini-hole event during the Arctic winter 2010/2011 as observed by SCIAMACHY and GOME-2. Atmospheric Chemistry and Physics, 2014, 14, 3247-3276.	1.9	29
300	Evolution of NO2 levels in Spain from 1996 to 2012. Scientific Reports, 2014, 4, 5887.	1.6	29
301	An exemplary case of a bromine explosion event linked to cyclone development in the Arctic. Atmospheric Chemistry and Physics, 2016, 16, 1773-1788.	1.9	29
302	Validation of Aura-OMI QA4ECV NO ₂ climate data records with ground-based DOAS networks: the role of measurement and comparison uncertainties. Atmospheric Chemistry and Physics, 2020, 20, 8017-8045.	1.9	29
303	Global total ozone recovery trends attributed to ozone-depleting substance (ODS) changes derived from five merged ozone datasets. Atmospheric Chemistry and Physics, 2022, 22, 6843-6859.	1.9	29
304	Room temperature rate coefficient for the reaction between CH3O2 and NO3. International Journal of Chemical Kinetics, 1990, 22, 673-681.	1.0	28
305	Trace gas and radical diurnal behavior in the marine boundary layer during INDOEX 1999. Journal of Geophysical Research, 2003, 108, .	3.3	28
306	Transport and build-up of tropospheric trace gases during the MINOS campaign: comparision of GOME, in situ aircraft measurements and MATCH-MPIC-data. Atmospheric Chemistry and Physics, 2003, 3, 1887-1902.	1.9	28

#	Article	IF	CITATIONS
307	The geostationary tropospheric pollution explorer (GeoTROPE) mission: objectives, requirements and mission concept. Advances in Space Research, 2004, 34, 682-687.	1.2	28
308	Pollution events over the East Mediterranean: Synergistic use of GOME, ground-based and sonde observations and models. Atmospheric Environment, 2007, 41, 7262-7273.	1.9	28
309	Technical Note: Characterisation of a DUALER instrument for the airborne measurement of peroxy radicals during AMMA 2006. Atmospheric Chemistry and Physics, 2010, 10, 3047-3062.	1.9	28
310	Improved stratospheric aerosol extinction profiles from SCIAMACHY: validation and sample results. Atmospheric Measurement Techniques, 2015, 8, 5223-5235.	1.2	28
311	Can a regional-scale reduction of atmospheric CO ₂ during the COVID-19 pandemic be detected from space? A case study for East China using satellite XCO ₂ retrievals. Atmospheric Measurement Techniques, 2021, 14, 2141-2166.	1.2	28
312	Rate coefficient for the reaction OH + HO2 = H2O + O2 at 1 atmosphere pressure and 308 K. Chemical Physics Letters, 1981, 84, 217-221.	1.2	27
313	DOAS Zenith Sky Observations: 1. BrO Measurements over Bremen (53°N) 1993–1994. Journal of Atmospheric Chemistry, 1997, 26, 93-108.	1.4	27
314	The impact of natural non-methane hydrocarbon oxidation on the free radical and ozone budgets above a eucalyptus forest. Chemosphere, 2001, 3, 353-366.	1.2	27
315	Ozone depletion observed by the Airborne Submillimeter Radiometer (ASUR) during the Arctic winter 1999/2000. Journal of Geophysical Research, 2002, 107, SOL 19-1.	3.3	27
316	Fast weighting functions for retrievals from limb scattering measurements. Journal of Quantitative Spectroscopy and Radiative Transfer, 2003, 77, 273-283.	1.1	27
317	Latitudinal variation of NLC particle radii derived from northern hemisphere SCIAMACHY/Envisat limb measurements. Advances in Space Research, 2007, 40, 765-771.	1.2	27
318	The influence of broken cloudiness on cloud top height retrievals using nadir observations of backscattered solar radiation in the oxygen A-band. Journal of Quantitative Spectroscopy and Radiative Transfer, 2007, 103, 460-477.	1.1	27
319	Assimilation of SCIAMACHY total column CO observations: Global and regional analysis of data impact. Journal of Geophysical Research, 2009, 114, .	3.3	27
320	Seasonality of halogen deposition in polar snow and ice. Atmospheric Chemistry and Physics, 2014, 14, 9613-9622.	1.9	27
321	Computation and analysis of atmospheric carbon dioxide annual mean growth rates from satellite observations during 2003–2016. Atmospheric Chemistry and Physics, 2018, 18, 17355-17370.	1.9	27
322	Severe Californian wildfires in November 2018 observed from space: the carbon monoxide perspective. Atmospheric Chemistry and Physics, 2020, 20, 3317-3332.	1.9	27
323	Rate coefficient for the reaction between NO3 radicals and dimethyl sulphide. Chemical Physics Letters, 1986, 130, 463-466.	1.2	26
324	The near-infrared bands of NO2 observed by high-resolution Fourier-transform spectroscopy. Journal of Chemical Physics, 1998, 109, 10217-10221.	1.2	26

#	Article	IF	CITATIONS
325	Systematic analysis of tropospheric NO ₂ long-range transport events detected in GOME-2 satellite data. Atmospheric Chemistry and Physics, 2014, 14, 7367-7396.	1.9	26
326	The response of mesospheric NO to geomagnetic forcing in 2002–2012 as seen by SCIAMACHY. Journal of Geophysical Research: Space Physics, 2016, 121, 3603-3620.	0.8	26
327	Radiative transfer modeling through terrestrial atmosphere and ocean accounting for inelastic processes: Software package SCIATRAN. Journal of Quantitative Spectroscopy and Radiative Transfer, 2017, 194, 65-85.	1.1	26
328	Aerosol particle size distribution in the stratosphere retrieved from SCIAMACHY limb measurements. Atmospheric Measurement Techniques, 2018, 11, 2085-2100.	1.2	26
329	Retrieval of aerosol optical thickness for desert conditions using MERIS observations during the SAMUM campaign. Tellus, Series B: Chemical and Physical Meteorology, 2022, 61, 229.	0.8	25
330	First high-resolution BrO column retrievals from TROPOMI. Atmospheric Measurement Techniques, 2019, 12, 2913-2932.	1.2	25
331	Validation of ACE-FTS version 3.5 NO _{<i>y</i>} species profiles using correlative satellite measurements. Atmospheric Measurement Techniques, 2016, 9, 5781-5810.	1.2	25
332	<title>Scanning imaging absorption spectrometer for atmospheric chartography</title> ., 1991, , .		24
333	Retrieval of total water vapour column amounts from GOME/ERS-2 data. Advances in Space Research, 2002, 29, 1697-1702.	1.2	24
334	A transboundary transport episode of nitrogen dioxide as observed from GOME and its impact in the Alpine region. Atmospheric Chemistry and Physics, 2005, 5, 23-37.	1.9	24
335	Peroxy radical partitioning during the AMMA radical intercomparison exercise. Atmospheric Chemistry and Physics, 2010, 10, 10621-10638.	1.9	24
336	The SPARC water vapour assessment II: comparison of annual, semi-annual and quasi-biennial variations in stratospheric and lower mesospheric water vapour observed from satellites. Atmospheric Measurement Techniques, 2017, 10, 1111-1137.	1.2	24
337	Airborne remote sensing and in situ measurements of atmospheric CO ₂ to quantify point source emissions. Atmospheric Measurement Techniques, 2018, 11, 721-739.	1.2	24
338	Variability of nitrogen oxide emission fluxes and lifetimes estimated from Sentinel-5P TROPOMI observations. Atmospheric Chemistry and Physics, 2022, 22, 2745-2767.	1.9	24
339	Modulated photolysis of the ozone—water vapour system: kinetics of the reaction of OH with HO2. Journal of Photochemistry and Photobiology, 1981, 16, 147-168.	0.6	23
340	A study of the N2O5 equilibrium between 275 and 315 K and determination of the heat of formation of NO3. Chemical Physics Letters, 1985, 119, 193-198.	1.2	23
341	Intercomparison of NO, NO2, NOy, O3, and ROxmeasurements during the Oxidizing Capacity of the Tropospheric Atmosphere (OCTA) campaign 1993 at Izaña. Journal of Geophysical Research, 1998, 103, 13615-13634.	3.3	23
342	Retrieval And Monitoring of Atmospheric Trace Gas Concentrations in Nadir and Limb Geometry Using the Space-Borne Sciamachy Instrument. Environmental Monitoring and Assessment, 2006, 120, 65-77.	1.3	23

#	Article	IF	CITATIONS
343	Water vapour profiles from SCIAMACHY solar occultation measurements derived with an onion peeling approach. Atmospheric Measurement Techniques, 2010, 3, 523-535.	1.2	23
344	SCIAMACHY WFM-DOAS <i>X</i> CO ₂ : reduction of scattering related errors. Atmospheric Measurement Techniques, 2012, 5, 2375-2390.	1.2	23
345	Liquid water absorption and scattering effects in DOAS retrievals over oceans. Atmospheric Measurement Techniques, 2014, 7, 4203-4221.	1.2	23
346	Long-term time series of Arctic tropospheric BrO derived from UV–VIS satellite remote sensing and its relation to first-year sea ice. Atmospheric Chemistry and Physics, 2020, 20, 11869-11892.	1.9	23
347	Kinetics of the gas-phase reactions of OH with NO2 and with NO. Journal of the Chemical Society, Faraday Transactions 2, 1983, 79, 111.	1.1	22
348	UV-visible absorption cross sections of bromine nitrate determined by photolysis of BrONO2/Br2mixtures. Journal of Geophysical Research, 1998, 103, 3563-3570.	3.3	22
349	Measurements of peroxy radicals in a forested area of Portugal. Chemosphere, 2001, 3, 327-338.	1.2	22
350	Continuous monitoring of the high and persistent chlorine activation during the Arctic winter 1999/2000 by the GOME instrument on ERS-2. Journal of Geophysical Research, 2002, 107, SOL 3-1.	3.3	22
351	Air mass factor calculations for GOME measurements of lightning-produced NO2. Advances in Space Research, 2002, 29, 1685-1690.	1.2	22
352	Solar occultation with SCIAMACHY: algorithm description and first validation. Atmospheric Chemistry and Physics, 2005, 5, 1589-1604.	1.9	22
353	The semianalytical cloud retrieval algorithm for SCIAMACHY II. The application to MERIS and SCIAMACHY data. Atmospheric Chemistry and Physics, 2006, 6, 4129-4136.	1.9	22
354	Intercomparison of SCIAMACHY and SIM vis-IR irradiance over several solar rotational timescales. Astronomy and Astrophysics, 2011, 528, A67.	2.1	22
355	Synergetic cloud fraction determination for SCIAMACHY using MERIS. Atmospheric Measurement Techniques, 2011, 4, 319-337.	1.2	22
356	Transcontinental methane measurements: Part 2. Mobile surface investigation of fossil fuel industrial fugitive emissions. Atmospheric Environment, 2013, 74, 432-441.	1.9	22
357	Differences in satellite-derived NO x emission factors between Eurasian and North American boreal forest fires. Atmospheric Environment, 2015, 121, 55-65.	1.9	22
358	A Fast Atmospheric Trace Gas Retrieval for Hyperspectral Instruments Approximating Multiple Scattering—Part 2: Application to XCO2 Retrievals from OCO-2. Remote Sensing, 2017, 9, 1102.	1.8	22
359	Ensemble-based satellite-derived carbon dioxide and methane column-averaged dry-air mole fraction data sets (2003–2018) for carbon and climate applications. Atmospheric Measurement Techniques, 2020, 13, 789-819.	1.2	22
360	Pressure broadening of the lowest rotational transition of OH studied by laser magnetic resonance. Chemical Physics Letters, 1979, 65, 197-200.	1.2	21

#	Article	IF	CITATIONS
361	The UV-A and visible solar irradiance spectrum: inter-comparison of absolutely calibrated, spectrally medium resolution solar irradiance spectra from balloon- and satellite-borne measurements. Atmospheric Chemistry and Physics, 2005, 5, 1879-1890.	1.9	21
362	Measurements of desert dust optical characteristics at Porte au Sahara during SAMUM. Tellus, Series B: Chemical and Physical Meteorology, 2022, 61, 206.	0.8	21
363	SCIAMACHY WFM-DOAS XCO ₂ : comparison with CarbonTracker XCO ₂ focusing on aerosols and thin clouds. Atmospheric Measurement Techniques, 2012, 5, 1935-1952.	1.2	21
364	Temperature dependent ozone absorption cross section spectra measured with the GOME-2 FM3 spectrometer and first application in satellite retrievals. Atmospheric Measurement Techniques, 2013, 6, 1623-1632.	1.2	21
365	Estimates of free-tropospheric NO ₂ and HCHO mixing ratios derived from high-altitude mountain MAX-DOAS observations at midlatitudes and in the tropics. Atmospheric Chemistry and Physics, 2016, 16, 2803-2817.	1.9	21
366	Space-based observation of volcanic iodine monoxide. Atmospheric Chemistry and Physics, 2017, 17, 4857-4870.	1.9	21
367	A Fast Atmospheric Trace Gas Retrieval for Hyperspectral Instruments Approximating Multiple Scattering—Part 1: Radiative Transfer and a Potential OCO-2 XCO2 Retrieval Setup. Remote Sensing, 2017, 9, 1159.	1.8	21
368	XBAER-derived aerosol optical thickness from OLCI/Sentinel-3 observation. Atmospheric Chemistry and Physics, 2018, 18, 2511-2523.	1.9	21
369	The HO2 radical UV absorption spectrum measured by molecular modulation, UV/diode-array spectroscopy. Journal of Photochemistry and Photobiology A: Chemistry, 1991, 60, 1-10.	2.0	20
370	Actinic flux and photolysis frequency comparison computations using the model PHOTOGT. Journal of Atmospheric Chemistry, 1996, 24, 1-21.	1.4	20
371	SCIAMACHY limb measurements in the UV/Vis spectral region: first results. Advances in Space Research, 2004, 34, 775-779.	1.2	20
372	SCIAMACHY validation by aircraft remote sensing: design, execution, and first measurement results of the SCIA-VALUE mission. Atmospheric Chemistry and Physics, 2005, 5, 1273-1290.	1.9	20
373	The Cloud Phase Discrimination From a Satellite. IEEE Geoscience and Remote Sensing Letters, 2006, 3, 103-106.	1.4	20
374	Aerosol optical depth retrieval over snow using AATSR data. International Journal of Remote Sensing, 2013, 34, 5030-5041.	1.3	20
375	Effect of surface BRDF of various land cover types on geostationary observations of tropospheric NO ₂ . Atmospheric Measurement Techniques, 2014, 7, 3497-3508.	1.2	20
376	Investigating differences in DOAS retrieval codes using MAD-CAT campaign data. Atmospheric Measurement Techniques, 2017, 10, 955-978.	1.2	20
377	High-resolution airborne imaging DOAS measurements of NO ₂ above Bucharest during AROMAT. Atmospheric Measurement Techniques, 2017, 10, 1831-1857.	1.2	20
378	Increased aerosol content in the atmosphere over Ukraine during summer 2010. Atmospheric Measurement Techniques, 2018, 11, 2101-2118.	1.2	20

#	Article	IF	CITATIONS
379	Line Shift Investigations for Different Isotopomers of Carbon Monoxide. Journal of Molecular Spectroscopy, 1998, 190, 226-231.	0.4	19
380	lodine and mercury resonance lamps for kinetics experiments and their spectra in the far ultraviolet. Journal Physics D: Applied Physics, 2000, 33, 1588-1591.	1.3	19
381	Global column density retrievals of mesospheric and thermospheric Mg I and Mg II from SCIAMACHY limb and nadir radiance data. Journal of Geophysical Research, 2008, 113, .	3.3	19
382	Evaluation of balloon and satellite water vapour measurements in the Southern tropical and subtropical UTLS during the HIBISCUS campaign. Atmospheric Chemistry and Physics, 2009, 9, 5299-5319.	1.9	19
383	Quantification and mitigation of the impact of scene inhomogeneity on Sentinel-4 UVN UV-VIS retrievals. Atmospheric Measurement Techniques, 2012, 5, 1319-1331.	1.2	19
384	Validation of SCIAMACHY limb NO ₂ profiles using solar occultation measurements. Atmospheric Measurement Techniques, 2012, 5, 1059-1084.	1.2	19
385	Coupled ocean-atmosphere radiative transfer model in the framework of software package SCIATRAN: Selected comparisons to model and satellite data. Advances in Space Research, 2012, 49, 1728-1742.	1.2	19
386	Chemical ozone losses in Arctic and Antarctic polar winter/spring season derived from SCIAMACHY limb measurements 2002–2009. Atmospheric Chemistry and Physics, 2013, 13, 1809-1835.	1.9	19
387	Peroxy radical detection for airborne atmospheric measurements using absorption spectroscopy of NO ₂ . Atmospheric Measurement Techniques, 2014, 7, 1245-1257.	1.2	19
388	The Unusual Stratospheric Arctic Winter 2019/20: Chemical Ozone Loss From Satellite Observations and TOMCAT Chemical Transport Model. Journal of Geophysical Research D: Atmospheres, 2021, 126, e2020JD034386.	1.2	19
389	Formation of N2O in the photolysis/photoexcitation of NO, NO2 and air. Journal of Photochemistry and Photobiology A: Chemistry, 1992, 66, 291-312.	2.0	18
390	Intercomparison of Stratospheric Chemistry Models under Polar Vortex Conditions. Journal of Atmospheric Chemistry, 2003, 45, 51-77.	1.4	18
391	New Directions: New Developments in Satellite Capabilities for Probing the Chemistry of the Troposphere. Atmospheric Environment, 2003, 37, 2567-2570.	1.9	18
392	SCIAMACHY on ENVISAT: in-flight optical performance and first results. , 2004, , .		18
393	Retrieval of trace gas vertical columns from SCIAMACHY/ENVISAT near-infrared nadir spectra: first preliminary results. Advances in Space Research, 2004, 34, 809-814.	1.2	18
394	Intercomparison of cloud top altitudes as derived using GOME and ATSR-2 instruments onboard ERS-2. Remote Sensing of Environment, 2006, 102, 186-193.	4.6	18
395	Modulations of the 27 day solar rotation signal in stratospheric ozone from Scanning Imaging Absorption Spectrometer for Atmospheric Cartography (SCIAMACHY) (2003–2008). Journal of Geophysical Research, 2010, 115, .	3.3	18
396	Evaluation of stratospheric chlorine chemistry for the Arctic spring 2005 using modelled and measured OClO column densities. Atmospheric Chemistry and Physics, 2011, 11, 689-703.	1.9	18

#	Article	IF	CITATIONS
397	Solar Spectral Irradiance Variations in 240 – 1600 nm During the Recent Solar Cycles 21 – Physics, 2011, 272, 159-188.	23. Solar	18
398	Dynamically controlled ozone decline in the tropical mid-stratosphere observed by SCIAMACHY. Atmospheric Chemistry and Physics, 2019, 19, 767-783.	1.9	18
399	Dual ground-based MAX-DOAS observations in Vienna, Austria: Evaluation of horizontal and temporal NO2, HCHO, and CHOCHO distributions and comparison with independent data sets. Atmospheric Environment: X, 2020, 5, 100059.	0.8	18
400	Measurement of the absorption cross-section of peroxynitric acid between 210 and 330 nm in the range 253 – 298 K. Journal of Photochemistry and Photobiology A: Chemistry, 1989, 48, 17-32.	2.0	17
401	Analysis of the UV absorption spectrum of ClO: a comparative study of four methods for spectral computations. Journal of Quantitative Spectroscopy and Radiative Transfer, 1999, 62, 345-369.	1.1	17
402	The geostationary scanning imaging absorption spectrometer (GeoSCIA) as part of the geostationary tropospheric pollution explorer (GeoTROPE) mission: requirements, concepts and capabilities. Advances in Space Research, 2004, 34, 694-699.	1.2	17
403	Seasonal variations of magnesium atoms in the mesosphereâ€thermosphere. Geophysical Research Letters, 2008, 35, .	1.5	17
404	Spatial variations of atmospheric methane concentrations in China. International Journal of Remote Sensing, 2011, 32, 833-847.	1.3	17
405	Precise pointing knowledge for SCIAMACHY solar occultation measurements. Atmospheric Measurement Techniques, 2012, 5, 2867-2880.	1.2	17
406	Retrieval of nitric oxide in the mesosphere and lower thermosphere from SCIAMACHY limb spectra. Atmospheric Measurement Techniques, 2013, 6, 2521-2531.	1.2	17
407	Comparison of nitric oxide measurements in the mesosphere and lower thermosphere from ACE-FTS, MIPAS, SCIAMACHY, and SMR. Atmospheric Measurement Techniques, 2015, 8, 4171-4195.	1.2	17
408	AÂstudy of the approaches used to retrieve aerosol extinction, as applied to limb observations made by OSIRIS and SCIAMACHY. Atmospheric Measurement Techniques, 2018, 11, 3433-3445.	1.2	17
409	Merging of ozone profiles from SCIAMACHY, OMPS and SAGE II observations to study stratospheric ozone changes. Atmospheric Measurement Techniques, 2019, 12, 2423-2444.	1.2	17
410	Development of a small unmanned aircraft system to derive CO ₂ emissions of anthropogenic point sources. Atmospheric Measurement Techniques, 2021, 14, 153-172.	1.2	17
411	Optical detection of NO3 and NO2 in ?pure? HNO3 vapor, the liquid-phase decomposition of HNO3. International Journal of Chemical Kinetics, 1993, 25, 795-803.	1.0	16
412	Nadir, limb, and occultation measurements with SCIAMACHY. Advances in Space Research, 2002, 29, 1819-1824.	1.2	16
413	Semiannual NO2plumes during the monsoon transition periods over the central Indian Ocean. Geophysical Research Letters, 2004, 31, .	1.5	16
414	Influence of ozone and temperature climatology on the accuracy of satellite total ozone retrieval. Journal of Geophysical Research, 2007, 112, .	3.3	16

#	Article	IF	CITATIONS
415	Intercomparison of ozone profile measurements from ASUR, SCIAMACHY, MIPAS, OSIRIS, and SMR. Journal of Geophysical Research, 2007, 112, .	3.3	16
416	Space-borne measurements of mesospheric magnesium species – a retrieval algorithm and preliminary profiles. Atmospheric Chemistry and Physics, 2008, 8, 1963-1983.	1.9	16
417	Error budget analysis of SCIAMACHY limb ozone profile retrievals using the SCIATRAN model. Atmospheric Measurement Techniques, 2013, 6, 2825-2837.	1.2	16
418	On the hiatus in the acceleration of tropical upwelling since the beginning of the 21st century. Atmospheric Chemistry and Physics, 2014, 14, 12803-12814.	1.9	16
419	Atmospheric remote sensing constraints on direct sea-air methane flux from the 22/4b North Sea massive blowout bubble plume. Marine and Petroleum Geology, 2015, 68, 824-835.	1.5	16
420	Copernicus Climate Change Service (C3S) Global Satellite Observations of Atmospheric Carbon Dioxide and Methane. Advances in Astronautics Science and Technology, 2018, 1, 57-60.	0.5	16
421	The retrieval of ice cloud parameters from multi-spectral satellite observations of reflectance using a modified XBAER algorithm. Remote Sensing of Environment, 2018, 215, 128-144.	4.6	16
422	Detection and quantification of CH ₄ plumes using the WFM-DOAS retrieval on AVIRIS-NG hyperspectral data. Atmospheric Measurement Techniques, 2021, 14, 1267-1291.	1.2	16
423	Quantification of CH ₄ coal mining emissions in Upper Silesia by passive airborne remote sensing observations with the Methane Airborne MAPper (MAMAP) instrument during the CO ₂ and Methane (CoMet) campaign. Atmospheric Chemistry and Physics. 2021. 21. 17345-17371.	1.9	16
424	Overview: On the transport and transformation of pollutants in the outflow of major population centres $\hat{a} \in $ observational data from the EMeRGe European intensive operational period in summer 2017. Atmospheric Chemistry and Physics, 2022, 22, 5877-5924.	1.9	16
425	Photolysis of chlorine nitrate at 254 nm. The Journal of Physical Chemistry, 1988, 92, 4340-4348.	2.9	15
426	Application of a Gaussian Distribution Function To Describe Molecular UVâ^'Visible Absorption Continua. 2. The UV Spectra of RO2•Radicals. Journal of Physical Chemistry A, 1997, 101, 2561-2567.	1.1	15
427	Stratospheric methane profiles from SCIAMACHY solar occultation measurements derived with onion peeling DOAS. Atmospheric Measurement Techniques, 2011, 4, 2567-2577.	1.2	15
428	On the potential of the 2041–2047nm spectral region for remote sensing of atmospheric CO2 isotopologues. Journal of Quantitative Spectroscopy and Radiative Transfer, 2012, 113, 2009-2017.	1.1	15
429	Water vapour and methane coupling in the stratosphere observed using SCIAMACHY solar occultation measurements. Atmospheric Chemistry and Physics, 2018, 18, 4463-4476.	1.9	15
430	XCO ₂ retrieval for GOSAT and GOSAT-2 based on the FOCAL algorithm. Atmospheric Measurement Techniques, 2021, 14, 3837-3869.	1.2	15
431	Product formation in the association reaction of ClO with NO2 investigated by diode laser kinetic spectroscopy. International Journal of Chemical Kinetics, 1984, 16, 445-467.	1.0	14
432	Consistent interpretation of ground based and GOME BrO slant column data. Advances in Space Research, 2002, 29, 1655-1660.	1.2	14

#	Article	IF	CITATIONS
433	The geostationary scanning imaging absorption spectrometer (GeoSCIA) mission: requirements and capabilities. Advances in Space Research, 2002, 29, 1849-1859.	1.2	14
434	The Determination of Cloud Altitudes Using SCIAMACHY Onboard ENVISAT. IEEE Geoscience and Remote Sensing Letters, 2004, 1, 211-214.	1.4	14
435	Principal and independent components analysis of overlapping spectra in the context of multichannel time-resolved absorption spectroscopy. Spectrochimica Acta - Part A: Molecular and Biomolecular Spectroscopy, 2004, 60, 2673-2693.	2.0	14
436	The Geostationary Fourier Imaging Spectrometer (GeoFIS) as part of the Geostationary Tropospheric Pollution Explorer (GeoTroPE) mission: objectives and capabilities. Advances in Space Research, 2004, 34, 688-693.	1.2	14
437	Atmospheric methanol measurement using selective catalytic methanol to formaldehyde conversion. Atmospheric Chemistry and Physics, 2005, 5, 2787-2796.	1.9	14
438	Retrieval of stratospheric NO3vertical profiles from SCIAMACHY lunar occultation measurement over the Antarctic. Journal of Geophysical Research, 2005, 110, .	3.3	14
439	Information operator approach and iterative regularization methods for atmospheric remote sensing. Journal of Quantitative Spectroscopy and Radiative Transfer, 2007, 103, 340-350.	1.1	14
440	Multi-year comparison of stratospheric BrO vertical profiles retrieved from SCIAMACHY limb and ground-based UV-visible measurements. Atmospheric Measurement Techniques, 2009, 2, 273-285.	1.2	14
441	Cloud and surface classification using SCIAMACHY polarization measurement devices. Atmospheric Chemistry and Physics, 2009, 9, 1279-1288.	1.9	14
442	Sensitivity of equatorial mesopause temperatures to the 27â€day solar cycle. Geophysical Research Letters, 2012, 39, .	1.5	14
443	Retrieval of Terrestrial Plant Fluorescence Based on the In-Filling of Far-Red Fraunhofer Lines Using SCIAMACHY Observations. Frontiers in Environmental Science, 2015, 3, .	1.5	14
444	A study of the impact of spatial resolution on the estimation of particle matter concentration from the aerosol optical depth retrieved from satellite observations. International Journal of Remote Sensing, 2019, 40, 7084-7112.	1.3	14
445	A cloud identification algorithm over the Arctic for use with AATSR–SLSTR measurements. Atmospheric Measurement Techniques, 2019, 12, 1059-1076.	1.2	14
446	Measurement report: regional trends of stratospheric ozone evaluated using the MErged GRIdded Dataset of Ozone Profiles (MEGRIDOP). Atmospheric Chemistry and Physics, 2021, 21, 6707-6720.	1.9	14
447	Retrieval of aerosol optical properties using MERIS observations: Algorithm and some first results. Remote Sensing of Environment, 2017, 197, 125-140.	4.6	14
448	Global validation of SCIAMACHY limb ozone data (versions 2.9 and 3.0, IUP Bremen) using ozonesonde measurements. Atmospheric Measurement Techniques, 2015, 8, 3369-3383.	1.2	14
449	Matrix-isolation spectra of chlorine nitrate. Chemical Physics Letters, 1984, 107, 341-346.	1.2	13
450	Matrix isolation Fourier transform infrared study of the products of the reaction between chlorine oxide (ClO) and nitrogen dioxide. The Journal of Physical Chemistry, 1985, 89, 266-271.	2.9	13

#	Article	IF	CITATIONS
451	Discharge flow kinetic study of the reactions of nitrate radical with bromine, bromine monoxide, hydrogen bromide, and hydrogen chloride. The Journal of Physical Chemistry, 1989, 93, 8017-8021.	2.9	13
452	The cold Arctic winter 1995/96 as observed by GOME and HALOE: Tropospheric wave activity and chemical ozone loss. Quarterly Journal of the Royal Meteorological Society, 2002, 128, 1293-1319.	1.0	13
453	Effects of column density on l ₂ spectroscopy and a determination of l ₂ absorption cross section at 500 nm. Atmospheric Chemistry and Physics, 2006, 6, 2177-2191.	1.9	13
454	Global cloud top height and thermodynamic phase distributions as obtained by SCIAMACHY on ENVISAT. International Journal of Remote Sensing, 2007, 28, 4499-4507.	1.3	13
455	Determination of the cloud fraction in the SCIAMACHY ground scene using MERIS spectral measurements. International Journal of Remote Sensing, 2009, 30, 6151-6167.	1.3	13
456	Global Distribution of Cloud Top Height as Retrieved from SCIAMACHY Onboard ENVISAT Spaceborne Observations. Remote Sensing, 2011, 3, 836-844.	1.8	13
457	Retrieval of aerosol mass load (PM ₁₀) from MERIS/Envisat top of atmosphere spectral reflectance measurements over Germany. Atmospheric Measurement Techniques, 2011, 4, 523-534.	1.2	13
458	Relative drifts and biases between six ozone limb satellite measurements from the last decade. Atmospheric Measurement Techniques, 2015, 8, 4369-4381.	1.2	13
459	Detection of outflow of formaldehyde and glyoxal from the African continent to the Atlantic Ocean with a MAX-DOAS instrument. Atmospheric Chemistry and Physics, 2019, 19, 10257-10278.	1.9	13
460	The SPARC water vapour assessment II: profile-to-profile comparisons of stratospheric and lower mesospheric water vapour data sets obtained from satellites. Atmospheric Measurement Techniques, 2019, 12, 2693-2732.	1.2	13
461	On the retrieval of aerosol optical depth over cryosphere using passive remote sensing. Remote Sensing of Environment, 2020, 241, 111731.	4.6	13
462	Retrieval algorithm for densities of mesospheric and lower thermospheric metal atom and ion species from satellite-borne limb emission signals. Atmospheric Measurement Techniques, 2014, 7, 29-48.	1.2	13
463	Retrieving the availability of light in the ocean utilising spectral signatures of vibrational Raman scattering in hyper-spectral satellite measurements. Ocean Science, 2015, 11, 373-389.	1.3	13
464	Intercomparison of the influence of tropospheric clouds on UV-visible absorptions Detected during the NDSC Intercomparison Campaign at OHP in June 1996. Geophysical Research Letters, 1999, 26, 1169-1172.	1.5	12
465	Application of a modified DOAS method for total ozone retrieval from GOME data at high polar latitudes. Advances in Space Research, 2004, 34, 749-753.	1.2	12
466	Influence of stratospheric airmasses on tropospheric vertical O ₃ columns based on GOME (Global Ozone Monitoring) Tj ETQq0 0 and Physics, 2004, 4, 903-909.	0 rgBT /O	verlock 10 Tf
467	The Intercomparison of Top-of-Atmosphere Reflectivity Measured by MERIS and SCIAMACHY in the Spectral Range of 443–865 nm. IEEE Geoscience and Remote Sensing Letters, 2007, 4, 293-296.	1.4	12
468	The Intercomparison of Cloud Parameters Derived Using Multiple Satellite Instruments. IEEE	2.7	12

The Intercomparison of Cloud Parameters Derived Using Multiple Satelli Transactions on Geoscience and Remote Sensing, 2007, 45, 195-200. 468

#	Article	IF	CITATIONS
469	Revised temperature-dependent ozone absorption cross-section spectra (Bogumil et al.) measured with the SCIAMACHY satellite spectrometer. Atmospheric Measurement Techniques, 2013, 6, 3055-3065.	1.2	12
470	UTLS water vapour from SCIAMACHY limb measurementsV3.01 (2002–2012). Atmospheric Measurement Techniques, 2016, 9, 133-158.	1.2	12
471	Stratospheric CH ₄ and CO ₂ profiles derived from SCIAMACHY solar occultation measurements. Atmospheric Measurement Techniques, 2016, 9, 1485-1503.	1.2	12
472	Comparison of global datasets of sodium densities in the mesosphere and lower thermosphere from GOMOS, SCIAMACHY and OSIRIS measurements and WACCM model simulations from 2008 to 2012. Atmospheric Measurement Techniques, 2017, 10, 2989-3006.	1.2	12
473	The SPARC water vapour assessment II: comparison of stratospheric and lower mesospheric water vapour time series observed from satellites. Atmospheric Measurement Techniques, 2018, 11, 4435-4463.	1.2	12
474	Retrieval of O ₂ (¹ Σ) and O ₂ (¹ Δ) volume emission rates in the mesosphere and lower thermosphere using SCIAMACHY MLT limb scans. Atmospheric Measurement Techniques, 2018, 11, 473-487.	1.2	12
475	Comparison of tropospheric NO ₂ columns from MAX-DOAS retrievals and regional air quality model simulations. Atmospheric Chemistry and Physics, 2020, 20, 2795-2823.	1.9	12
476	Tropospheric Remote Sensing from Space. Physics of Earth and Space Environments, 2011, , 1-65.	0.5	12
477	The absorption spectrum of CINO between 190 and 350 nm. Journal of Photochemistry and Photobiology, 1987, 36, 133-139.	0.6	11
478	N2Broadening in the13C16O 2–0 Band around 4167 cmâ^'1. Journal of Molecular Spectroscopy, 1996, 180, 359-364.	0.4	11
479	Observations of the moon by the global ozone monitoring experiment: radiometric calibration and lunar albedo. Applied Optics, 1998, 37, 7832.	2.1	11
480	Global atmospheric monitoring with SCIAMACHY. Physics and Chemistry of the Earth, Part C: Solar, Terrestrial and Planetary Science, 1999, 24, 427-434.	0.2	11
481	Estimation of the emission temperature of an electrodeless discharge lamp and determination of the oscillator strength for the I(2P3/2) 183.038 nm resonance transition. Spectrochimica Acta, Part B: Atomic Spectroscopy, 2001, 56, 2465-2478.	1.5	11
482	Neural network scheme for the retrieval of total ozone from Global Ozone Monitoring Experiment data. Applied Optics, 2002, 41, 5051.	2.1	11
483	The SCIAMACHY calibration/monitoring concept and first results. Advances in Space Research, 2003, 32, 2123-2128.	1.2	11
484	The determination of the atmospheric optical thickness over Western Europe using SeaWiFS imagery. IEEE Transactions on Geoscience and Remote Sensing, 2004, 42, 824-832.	2.7	11
485	Trace gas column retrieval – an error assessment study for GOME-2. Advances in Space Research, 2004, 34, 727-733.	1.2	11
486	Satellite Ozone Retrieval Under Broken Cloud Conditions: An Error Analysis Based on Monte Carlo Simulations. IEEE Transactions on Geoscience and Remote Sensing, 2007, 45, 187-194.	2.7	11

#	Article	IF	CITATIONS
487	Sensitivity of polar stratospheric cloud formation to changes in water vapour and temperature. Atmospheric Chemistry and Physics, 2016, 16, 101-121.	1.9	11
488	Tropospheric ozone maxima observed over the Arabian Sea during the pre-monsoon. Atmospheric Chemistry and Physics, 2017, 17, 4915-4930.	1.9	11
489	The New SCIAMACHY Reference Solar Spectral Irradiance and Its Validation. Solar Physics, 2018, 293, 1.	1.0	11
490	Stratospheric aerosol characteristics from space-borne observations: extinction coefficient and Ãngström exponent. Atmospheric Measurement Techniques, 2019, 12, 3485-3502.	1.2	11
491	Retrieval of Aerosol Optical Thickness in the Arctic Snow-Covered Regions Using Passive Remote Sensing: Impact of Aerosol Typing and Surface Reflection Model. IEEE Transactions on Geoscience and Remote Sensing, 2020, 58, 5117-5131.	2.7	11
492	SCIAMACHY's View of the Changing Earth's Environment. , 2011, , 175-216.		11
493	Interpretation of Mid-Stratospheric Arctic Ozone Measurements Using a Photochemical Box-Model. Journal of Atmospheric Chemistry, 1999, 34, 281-290.	1.4	10
494	First results of ozone profiles between 35 and 65km retrieved from SCIAMACHY limb spectra and observations of ozone depletion during the solar proton events in October/November 2003. Advances in Space Research, 2006, 37, 2263-2268.	1.2	10
495	Calibration of SCIAMACHY Using AATSR Top-of-Atmosphere Reflectance Over a Hurricane. IEEE Geoscience and Remote Sensing Letters, 2007, 4, 8-12.	1.4	10
496	Markov chain analysis of regional climates. Nonlinear Processes in Geophysics, 2010, 17, 651-661.	0.6	10
497	A case study on the application of SCIAMACHY satellite methane measurements for regional studies: the Greater Area of the Eastern Mediterranean. International Journal of Remote Sensing, 2011, 32, 787-813.	1.3	10
498	Impacts of the January 2005 solar particle event on noctilucent clouds and water at the polar summer mesopause. Atmospheric Chemistry and Physics, 2012, 12, 5633-5646.	1.9	10
499	Diel peroxy radicals in a semi-industrial coastal area: nighttime formation of free radicals. Atmospheric Chemistry and Physics, 2013, 13, 5731-5749.	1.9	10
500	Understanding MODIS dark-target collection 5 and 6 aerosol data over China: Effect of surface type, aerosol loading and aerosol absorption. Atmospheric Research, 2019, 228, 161-175.	1.8	10
501	Systematic comparison of vectorial spherical radiative transfer models in limb scattering geometry. Atmospheric Measurement Techniques, 2021, 14, 3953-3972.	1.2	10
502	Validation strategy for satellite observations of tropospheric reactive gases. Annals of Geophysics, 2014, , .	0.5	10
503	Retrieval of greenhouse gases from GOSAT and GOSAT-2 using the FOCAL algorithm. Atmospheric Measurement Techniques, 2022, 15, 3401-3437.	1.2	10
504	Lunar occultation with SCIAMACHY: First retrieval results. Advances in Space Research, 2005, 36, 906-914.	1.2	9

#	Article	IF	CITATIONS
505	Corrigendum to "First direct observation of the atmospheric CO ₂ year-to-year increase from space" published in Atmos. Chem. Phys., 7, 4249–4256, 2007. Atmospheric Chemistry and Physics, 2007, 7, 5341-5342.	1.9	9
506	Investigation of Solar Irradiance Variations and Their Impact on Middle Atmospheric Ozone. Springer Atmospheric Sciences, 2013, , 39-54.	0.4	9
507	Investigating missing sources of glyoxal over China using a regional air quality model (RAMS-CMAQ). Journal of Environmental Sciences, 2018, 71, 108-118.	3.2	9
508	Harmonisation and trends of 20-year tropical tropospheric ozone data. Atmospheric Chemistry and Physics, 2018, 18, 9189-9205.	1.9	9
509	Near-surface and path-averaged mixing ratios of NO ₂ derived from car DOAS zenith-sky and tower DOAS off-axis measurements in Vienna: a case study. Atmospheric Chemistry and Physics, 2019, 19, 5853-5879.	1.9	9
510	Estimation of ship emission rates at a major shipping lane by long-path DOAS measurements. Atmospheric Measurement Techniques, 2021, 14, 5791-5807.	1.2	9
511	Ozone profile retrieval from nadir TROPOMI measurements in the UV range. Atmospheric Measurement Techniques, 2021, 14, 6057-6082.	1.2	9
512	Studies of the horizontal inhomogeneities in NO ₂ concentrations above a shipping lane using ground-based multi-axis differential optical absorption spectroscopy (MAX-DOAS) measurements and validation with airborne imaging DOAS measurements. Atmospheric Measurement Techniques, 2019, 12, 5959-5977.	1.2	9
513	A study of the formation of N2O in the reaction of NO3(A2E′) with N2. Journal of Atmospheric Chemistry, 1992, 15, 157-169.	1.4	8
514	<title>SCIAMACHY instrument on ENVISAT-1</title> ., 1998, 3498, 94.		8
515	New High-Resolution Analysis of the ν3 Band of the 15N16O2 Isotopomer of Nitrogen Dioxide by Fourier Transform Spectroscopy. Journal of Molecular Spectroscopy, 2000, 204, 72-79.	0.4	8
516	Ozone depletion in Northern Hemisphere winter/spring 1999/2000 as measured by the Global Ozone Monitoring Experiment on ERS-2. Journal of Geophysical Research, 2002, 107, SOL 23-1.	3.3	8
517	Time-windowing Fourier transform absorption spectroscopy for flash photolysis investigations. Journal of Photochemistry and Photobiology A: Chemistry, 2003, 157, 127-136.	2.0	8
518	Towards O3 and NO2 vertical profile retrieval from SCIAMACHY solar occultation measurements: first results. Advances in Space Research, 2004, 34, 744-748.	1.2	8
519	Measurements of O ₃ , NO ₂ and BrO during the INDOEX campaign using ground based DOAS and GOME satellite data. Atmospheric Chemistry and Physics, 2007, 7, 283-291.	1.9	8
520	First CRDS-measurements of water vapour continuum in the 940nm absorption band. Journal of Quantitative Spectroscopy and Radiative Transfer, 2007, 105, 303-311.	1.1	8
521	The sensitivity of Western European NO ₂ columns to interannual variability of meteorology and emissions: a model—GOME study. Atmospheric Science Letters, 2008, 9, 182-188.	0.8	8
522	Comparison of NLC particle sizes derived from SCIAMACHY/Envisat observations with ground-based LIDAR measurements at ALOMAR (69° N). Atmospheric Measurement Techniques, 2009, 2, 523-531.	1.2	8

#	Article	IF	CITATIONS
523	Metal concentrations in the upper atmosphere during meteor showers. Atmospheric Chemistry and Physics, 2010, 10, 909-917.	1.9	8
524	Ship track characteristics derived from geostationary satellite observations on the west coast of southern Africa. Atmospheric Research, 2010, 95, 32-39.	1.8	8
525	Impact of solar proton events on noctilucent clouds. Journal of Atmospheric and Solar-Terrestrial Physics, 2011, 73, 2073-2081.	0.6	8
526	Frequency stabilization of blue extended cavity diode lasers by external cavity optical feedback. Applied Physics B: Lasers and Optics, 2012, 106, 261-266.	1.1	8
527	Retrieval of nitric oxide in the mesosphere from SCIAMACHY nominal limb spectra. Atmospheric Measurement Techniques, 2017, 10, 209-220.	1.2	8
528	A Critical Evaluation of Deep Blue Algorithm Derived AVHRR Aerosol Product Over China. Journal of Geophysical Research D: Atmospheres, 2019, 124, 12173-12193.	1.2	8
529	Retrieval of Particulate Matter from MERIS Observations. , 2008, , 190-202.		8
530	On the influence of underlying elevation data on Sentinel-5 Precursor TROPOMI satellite methane retrievals over Greenland. Atmospheric Measurement Techniques, 2022, 15, 4063-4074.	1.2	8
531	Sciamachy instrument design. Advances in Space Research, 1991, 11, 243-246.	1.2	7
532	<title>SCIAMACHY on-ground/in-flight calibration, performance verification, and monitoring concepts</title> . , 1997, , .		7
533	Development of a correlated-k distribution band model scheme for the radiative transfer program GOMETRAN/SCIATRAN for retrieval of atmospheric constituents from SCIMACHY/ENVISAT-1 data. , 1998, , .		7
534	Current and future passive remote sensing techniques used to determine atmospheric constitutents. Developments in Atmospheric Science, 1999, , 317-347.	0.3	7
535	Satellite measurements of the atmospheric content of metallic ion and neutral species. Advances in Space Research, 2004, 33, 1481-1485.	1.2	7
536	The Visible Absorption Spectrum of OBrO, Investigated by Fourier Transform Spectroscopy. Journal of Physical Chemistry A, 2005, 109, 5093-5103.	1.1	7
537	Global cloud top height retrieval using SCIAMACHY limb spectra: model studies and first results. Atmospheric Measurement Techniques, 2016, 9, 793-815.	1.2	7
538	Tropical tropospheric ozone columns from nadir retrievals of GOME-1/ERS-2, SCIAMACHY/Envisat, and GOME-2/MetOp-A (1996–2012). Atmospheric Measurement Techniques, 2016, 9, 3407-3427.	1.2	7
539	Evaluation of SCIAMACHY ESA/DLR Cloud Parameters Version 5.02 by Comparisons to Ground-Based and Other Satellite Data. Frontiers in Environmental Science, 2016, 4, .	1.5	7
540	First mesopause Na retrievals from satellite Na Dâ€line nightglow observations. Geophysical Research Letters, 2016, 43, 12,651.	1.5	7

#	Article	IF	CITATIONS
541	In-flight calibration of SCIAMACHY's polarization sensitivity. Atmospheric Measurement Techniques, 2018, 11, 265-289.	1.2	7
542	A fast and accurate radiative transfer model for aerosol remote sensing. Journal of Quantitative Spectroscopy and Radiative Transfer, 2020, 256, 107270.	1.1	7
543	Implementation of an ice crystal single-scattering property database in the radiative transfer model SCIATRAN. Journal of Quantitative Spectroscopy and Radiative Transfer, 2020, 253, 107118.	1.1	7
544	The retrieval of snow properties from SLSTR Sentinel-3 – Part 2: Results and validation. Cryosphere, 2021, 15, 2781-2802.	1.5	7
545	Changes in stratospheric aerosol extinction coefficient after the 2018ÂAmbae eruption as seen by OMPS-LP and MAECHAM5-HAM. Atmospheric Chemistry and Physics, 2021, 21, 14871-14891.	1.9	7
546	Combined UV and IR ozone profile retrieval from TROPOMI and CrIS measurements. Atmospheric Measurement Techniques, 2022, 15, 2955-2978.	1.2	7
547	O3 profiles from GOME satellite data—I: Comparison with ozonesonde measurements. Physics and Chemistry of the Earth, Part C: Solar, Terrestrial and Planetary Science, 1999, 24, 447-452.	0.2	6
548	GOME ozone profiles: a global validation with HALOE measurements. Advances in Space Research, 2002, 29, 1637-1642.	1.2	6
549	Impact of Accurate Photolysis Calculations on the Simulation of Stratospheric Chemistry. Journal of Atmospheric Chemistry, 2003, 44, 225-240.	1.4	6
550	In-flight calibration of the SCIAMACHY solar irradiance spectrum. Advances in Space Research, 2003, 32, 2129-2134.	1.2	6
551	Ozone profile retrieval from limb scatter measurements in the HARTLEY bands: further retrieval details and profile comparisons. Atmospheric Chemistry and Physics, 2008, 8, 2509-2517.	1.9	6
552	Polarization data from SCIAMACHY limb backscatter observations compared to vector radiative transfer model simulations. Atmospheric Measurement Techniques, 2013, 6, 1503-1520.	1.2	6
553	The fractal perimeter dimension of noctilucent clouds: Sensitivity analysis of the area–perimeter method and results on the seasonal and hemispheric dependence of the fractal dimension. Journal of Atmospheric and Solar-Terrestrial Physics, 2015, 127, 66-72.	0.6	6
554	Polarized radiative transfer through terrestrial atmosphere accounting for rotational Raman scattering. Journal of Quantitative Spectroscopy and Radiative Transfer, 2017, 200, 70-89.	1.1	6
555	Airborne measurement of peroxy radicals using chemical amplification coupled with cavity ring-down spectroscopy: the PeRCEAS instrument. Atmospheric Measurement Techniques, 2020, 13, 2577-2600.	1.2	6
556	The retrieval of snow properties from SLSTR Sentinel-3 – Part 1: Method description and sensitivity study. Cryosphere, 2021, 15, 2757-2780.	1.5	6
557	Ten-Year SCIAMACHY Stratospheric Aerosol Data Record: Signature of the Secondary Meridional Circulation Associated with the Quasi-Biennial Oscillation. Springer Earth System Sciences, 2015, , 49-58.	0.1	6
558	<title>SCIAMACHY: a new generation of hyperspectral remote sensing instrument</title> ., 1997, , .		6

#	Article	IF	CITATIONS
559	Spatial distribution of enhanced BrO and its relation to meteorological parameters in Arctic and Antarctic sea ice regions. Atmospheric Chemistry and Physics, 2020, 20, 12285-12312.	1.9	6
560	Intracavity diode laser for atmospheric field measurements. Infrared Physics and Technology, 1996, 37, 95-98.	1.3	5
561	O3 Profiles from GOME satellite data—ll: Observations in the Arctic Spring 1997 and 1998. Physics and Chemistry of the Earth, Part C: Solar, Terrestrial and Planetary Science, 1999, 24, 453-457.	0.2	5
562	Theoretical precisions for sciamachy limb retrieval. Advances in Space Research, 2002, 29, 1837-1842.	1.2	5
563	SCIAMACHY limb spectra. Advances in Space Research, 2004, 34, 715-720.	1.2	5
564	UV limb-scatter spectra of noctilucent clouds consistent with mono-modal particle size distribution. Geophysical Research Letters, 2007, 34, .	1.5	5
565	Towards validation of SCIAMACHY lunar occultation NO2 vertical profiles. Advances in Space Research, 2008, 41, 1921-1932.	1.2	5
566	A feasibility study for the detection of the diurnal variation of tropospheric NO2 over Tokyo from a geostationary orbit. Advances in Space Research, 2011, 48, 1551-1564.	1.2	5
567	SCIAMACHY lunar occultation water vapor measurements: retrieval and validation results. Atmospheric Measurement Techniques, 2012, 5, 2499-2513.	1.2	5
568	Retrieval of sodium number density profiles in the mesosphere and lower thermosphere from SCIAMACHY limb emission measurements. Atmospheric Measurement Techniques, 2016, 9, 295-311.	1.2	5
569	GOME-2A retrievals of tropospheric NO ₂ in different spectral ranges – influence of penetration depth. Atmospheric Measurement Techniques, 2018, 11, 2769-2795.	1.2	5
570	Full-azimuthal imaging-DOAS observations of NO ₂ and O ₄ during CINDI-2. Atmospheric Measurement Techniques, 2019, 12, 4171-4190.	1.2	5
571	Extending XBAER Algorithm to Aerosol and Cloud Condition. IEEE Transactions on Geoscience and Remote Sensing, 2019, 57, 8262-8275.	2.7	5
572	Global diffuse attenuation derived from vibrational Raman scattering detected in hyperspectral backscattered satellite spectra. Optics Express, 2019, 27, A829.	1.7	5
573	Total water vapour columns derived from Sentinel 5P using the AMC-DOAS method. Atmospheric Measurement Techniques, 2022, 15, 297-320.	1.2	5
574	A preliminary comparison between TOVS and GOME level 2 ozone data. Geophysical Research Letters, 1997, 24, 2191-2194.	1.5	4
575	Atmospheric trace gas sounding with SCIAMACHY. Advances in Space Research, 2000, 26, 1949-1954.	1.2	4
576	Evaluation of the combined differential-integral approach for limb viewing geometry. Advances in Space Research, 2002, 29, 1843-1848.	1.2	4

#	Article	IF	CITATIONS
577	Long-term global measurements of ozone profiles by GOME validated with SAGE II considering atmospheric dynamics. Journal of Geophysical Research, 2004, 109, .	3.3	4
578	Quantitative treatment of coarsely binned low-resolution recordings in molecular absorption spectroscopy. Spectrochimica Acta - Part A: Molecular and Biomolecular Spectroscopy, 2006, 64, 722-735.	2.0	4
579	Remote sensing atmospheric trace gases with infrared imaging spectroscopy. Eos, 2012, 93, 525-525.	0.1	4
580	Simulated air quality and pollutant budgets over Europe in 2008. Science of the Total Environment, 2014, 470-471, 270-281.	3.9	4
581	Comparison of ground-based and satellite measurements of water vapour vertical profiles over Ellesmere Island, Nunavut. Atmospheric Measurement Techniques, 2019, 12, 4039-4063.	1.2	4
582	Mesospheric nitric oxide model from SCIAMACHY data. Atmospheric Chemistry and Physics, 2019, 19, 2135-2147.	1.9	4
583	Validation of GOME ozone profiles by means of the ALOMAR ozone lidar. Annales Geophysicae, 2003, 21, 1879-1886.	0.6	4
584	A new snow bidirectional reflectance distribution function model in spectral regions from UV to SWIR: Model development and application to ground-based, aircraft and satellite observations. ISPRS Journal of Photogrammetry and Remote Sensing, 2022, 188, 269-285.	4.9	4
585	The SPARC Water Vapor Assessment II: assessment of satellite measurements of upper tropospheric humidity. Atmospheric Measurement Techniques, 2022, 15, 3377-3400.	1.2	4
586	Gas phase spectra of HOBr and Br2O and their atmospheric significance. Annales Geophysicae, 1996, 14, 468-475.	0.6	3
587	Retrieval of spectral aerosol optical thickness from multi-wavelength space-borne sensors. Advances in Space Research, 2002, 29, 1765-1770.	1.2	3
588	Improvements in the tropical ozone profile retrieval from GOME-UV/Vis nadir spectra. Advances in Space Research, 2004, 34, 739-743.	1.2	3
589	Carbon monoxide spatial gradients over source regions as observed by SCIAMACHY: A case study for the United Kingdom. Advances in Space Research, 2009, 43, 923-929.	1.2	3
590	Determination of Cloud Optical Thickness Over Snow Using Satellite Measurements in the Oxygen A-Band. IEEE Geoscience and Remote Sensing Letters, 2013, 10, 1162-1166.	1.4	3
591	Simulated reflectance above snow constrained by airborne measurements of solar radiation: implications for the snow grain morphology in the Arctic. Atmospheric Measurement Techniques, 2021, 14, 369-389.	1.2	3
592	Modeling of inelastically scattered radiation: Rotational Raman scattering in the spherical Earth's atmosphere. Journal of Quantitative Spectroscopy and Radiative Transfer, 2021, 268, 107611.	1.1	3
593	Ambient Radical Concentrations in the Presence of Airborne Liquid Water. , 1986, , 351-366.		3
			_

594 Satellite Observations of Tropospheric and Stratospheric Gases. , 2000, , 301-329.

#	ARTICLE	IF	CITATIONS
595	Validation of XCO ₂ and XCH ₄ retrieved from a portable Fourier transform spectrometer with those from in situ profiles from aircraft-borne instruments. Atmospheric Measurement Techniques, 2020, 13, 5149-5163.	1.2	3
596	<title>GOME instrument simulation</title> ., 1993,,.		2
597	Ozone profile distributions in the Arctic from GOME satellite observations during spring 1997 and 1998, , .		2
598	GODIVA, a European project for ozone and trace gas measurements from gome. Advances in Space Research, 2000, 26, 951-954.	1.2	2
599	Temporal evolution of the vertical content of metallic ion and neutral species. Journal of Atmospheric and Solar-Terrestrial Physics, 2005, 67, 1238-1244.	0.6	2
600	A Graduate-Level Online Module for Teaching Remote Sensing of Tropospheric NO2 from Space. Journal of Chemical Education, 2009, 86, 750.	1.1	2
601	A New Method for the Comparison of Trend Data with an Application to Water Vapor. Journal of Climate, 2011, 24, 3124-3141.	1.2	2
602	Improved pointing information for SCIAMACHY from in-flight measurements of the viewing directions towards sun and moon. Atmospheric Measurement Techniques, 2017, 10, 2413-2423.	1.2	2
603	Concept of small satellite UV/visible imaging spectrometer optimized for tropospheric NO2 measurements in air quality monitoring. Acta Astronautica, 2019, 160, 421-432.	1.7	2
604	Retrieval of aerosol optical thickness and surface parameters based on multi-spectral and multi-viewing space-borne measurements. Journal of Quantitative Spectroscopy and Radiative Transfer, 2020, 256, 107311.	1.1	2
605	On the use of satellite observations to fill gaps in the Halley station total ozone record. Atmospheric Chemistry and Physics, 2021, 21, 9829-9838.	1.9	2
606	Total ozone column from Ozone Mapping and Profiler Suite Nadir Mapper (OMPS-NM) measurements using the broadband weighting function fitting approach (WFFA). Atmospheric Measurement Techniques, 2021, 14, 5771-5789.	1.2	2
607	SCIAMACHY Solar Occultation: Ozone and NO2 Profiles 2002–2007. , 2009, , 79-86.		2
608	Studies of NO2 from Lightning and Convective Uplifting using GOME Data. , 2004, , 297-306.		2
609	Perspectives and Integration in SOLAS Science. Springer Earth System Sciences, 2014, , 247-306.	0.1	2
610	Laboratory Studies of Peroxy Radicals, Carbonyl Compounds and Ozonolysis Reactions of Tropospheric Importance. , 1997, , 162-169.		2
611	Impact of Short-Term Solar Variability on the Polar Summer Mesopause and Noctilucent Clouds. Springer Atmospheric Sciences, 2013, , 365-382.	0.4	2
612	Room Temperature Rate Coefficient for the Reaction between CH3O2 and NO3. , 1990, , 371-376.		2

Room Temperature Rate Coefficient for the Reaction between CH3O2 and NO3., 1990, , 371-376. 612

#	Article	IF	CITATIONS
613	A TTFM Spectrometer for Detection of Transient Radical Species: 2Ï 1 Overtone Absorption Lines of Ho2 AT 1.5 μm. , 1992, , 183-190.		2
614	Retrieval of aerosol optical thickness for desert conditions using MERIS observations during the SAMUM campaign. Tellus, Series B: Chemical and Physical Meteorology, 2009, 61, .	0.8	2
615	Sounding The Troposphere From Space: A New Era For Global Atmospheric Chemistry. NATO Science for Peace and Security Series C: Environmental Security, 2008, , 173-200.	0.1	2
616	GOME satellite detection of ozone over a snow/ice covered surface in the presence of broken clouds. , 2002, 4539, 79.		1
617	Trace gas column retrieval from IR nadir spectra – a model study for SCIAMACHY. Advances in Space Research, 2004, 34, 734-738.	1.2	1
618	Aerosol retrieval over land surfaces from multispectral nadir looking satellite measurements. , 2004, 5235, 366.		1
619	Global mapping of greenhouse gases and air pollutants. Europhysics News, 2007, 38, 26-32.	0.1	1
620	Corrigendum to "Spectral studies of ocean water with space-borne sensor SCIAMACHY using Differential Optical Absorption Spectroscopy (DOAS)" published in Ocean Sci., 3, 429–440, 2007. Ocean Science, 2007, 3, 483-483.	1.3	1
621	Nine years of atmospheric remote sensing with sciamachy - atmospheric parameters and data products. , 2011, , .		1
622	A study of BRDF over Tokyo for the spaceborne measurements of atmospheric trace gases. , 2012, , .		1
623	Earth observation: a revolutionary leap into the future. Astronomy and Geophysics, 2012, 53, 3.16-3.18.	0.1	1
624	The greenhouse gas project of ESA's climate change initiative (GHG-CCI): overview, achievements and future plans. International Archives of the Photogrammetry, Remote Sensing and Spatial Information Sciences - ISPRS Archives, 0, XL-7/W3, 165-172.	0.2	1
625	Reduced Methane Emissions from Santa Barbara Marine Seeps. Remote Sensing, 2017, 9, 1162.	1.8	1
626	Remote Sensing of Tropospheric Trace Gases (NO2 and SO2) from SCIAMACHY. , 2009, , 63-72.		1
627	Investigating the Link Between Glyoxal and Biogenic Activities. Springer Earth System Sciences, 2015, , 59-65.	0.1	1
628	Laboratory and Field Measurement Studies of the Tropospheric Chemistry of Nitrate and Peroxy Radicals. , 1997, , 91-99.		1
629	Data Assimilation and Model Calculations to Study Chemistry Climate Interactions in the Stratosphere. Springer Atmospheric Sciences, 2013, , 149-170.	0.4	1
630	Validation of ozone profiles from GOME satellite data. , 1998, , .		1

630 Validation of ozone profiles from GOME satellite data. , 1998, , .

#	Article	IF	CITATIONS
631	Optimised degradation correction for SCIAMACHY satellite solar measurements from 330 to 1600 nm by using the internal white light source. Atmospheric Measurement Techniques, 2020, 13, 3893-3907.	1.2	1
632	Stratospheric aerosol extinction profiles from SCIAMACHY solar occultation. Atmospheric Measurement Techniques, 2020, 13, 5643-5666.	1.2	1
633	Simulating tropospheric BrO in the Arctic using an artificial neural network. Atmospheric Environment, 2022, 276, 119032.	1.9	1
634	External resonator tunable diode laser (TDL) system for extracavity and intracavity absorption: experiments and modeling. , 1996, 2834, 24.		0
635	Estimation of spectral aerosol optical thickness during indoex from SeaWIFS radiance. Journal of Aerosol Science, 2000, 31, 289-290.	1.8	0
636	A cloud retrieval algorithm for SCIAMACHY. , 2003, 5059, 116.		0
637	SCIAMACHY on ENVISAT: instrument monitoring and calibration two years after launch. , 2004, , .		0
638	The Visible Absorption Spectrum of OBrO, Investigated by Fourier Transform Spectroscopy ChemInform, 2005, 36, no.	0.1	0
639	SCIAMACHY on ENVISAT: 4 Years in Space: A Status Report. , 2006, , .		0
640	Session A1.1. Atmospheric Remote Sensing: Earth's Surface, Troposphere, Stratosphere and Mesosphere – Second volume. Advances in Space Research, 2006, 37, 2149.	1.2	0
641	Sensitivity Study of the Airmass Factors used for Satellite Retrievals of tropospheric NO2. , 2009, , .		0
642	Corrigendum to ''Peroxy radical observations over West Africa during AMMA 2006: photochemical activity in the outflow of convective systems" published in Atmos. Chem. Phys., 9, 3681–3695, 2009. Atmospheric Chemistry and Physics, 2009, 9, 8103-8104.	1.9	0
643	A brief introduction and some background to the article JQSRT 1998;60:1025–31 and its companion. Journal of Quantitative Spectroscopy and Radiative Transfer, 2010, 111, 1841-1844.	1.1	0
644	Corrigendum to "Trend analysis of aerosol optical thickness and Ångström exponent derived from the global AERONET spectral observations" published in Atmos. Meas. Tech., 5, 1271–1299, 2012. Atmospheric Measurement Techniques, 2012, 5, 2113-2113.	1.2	0
645	Corrigendum to "Simultaneous satellite observations of IO and BrO over Antarctica" published in Atmos. Chem. Phys., 12, 6565–6580, 2012. Atmospheric Chemistry and Physics, 2012, 12, 9383-9385.	1.9	0
646	Quantification of Tropospheric Measurements from Nadir Viewing UV/Visible Instruments. , 2004, , 137-147.		0
647	Towards Operational Monitoring of the Chemical Composition of the Atmosphere Using Solar Backscatter Imaging Techniques. , 2007, , .		0
648	Satellite Monitoring of Nitrogen Oxide Emissions. NATO Science for Peace and Security Series C: Environmental Security, 2011, , 219-234.	0.1	0

#	Article	IF	CITATIONS
649	Individual Reports from JETDLAG Contributors. , 1997, , 237-297.		Ο
650	Chemical ozone loss in the Arctic vortex in the winter 1995–96: HALOE measurements in conjunction with other observations. Annales Geophysicae, 1999, 17, 101.	0.6	0
651	Estimates of NOx Emission Factors from GOME-2 Measurements for the Major Types of Open Biomass Burning. Springer Earth System Sciences, 2015, , 67-75.	0.1	Ο
652	Towards a Better Tropospheric Ozone Data Product from SCIAMACHY: Improvements in High Latitude Stratospheric Ozone. Springer Earth System Sciences, 2015, , 39-48.	0.1	0
653	TIBAGS: Tropospheric Iodine Monoxide and Its Coupling to Biospheric and Atmospheric Variables—a Global Satellite Study. Springer Earth System Sciences, 2016, , 15-34.	0.1	Ο
654	Using Passive Remote Sensing in the Short Wave Infrared to Quantify Methane and CO2 Point Source Emissions. , 2016, , .		0